U.PORTO
FACULDADE DE CIÊNCIAS
UNIVERSIDADE DO PORTO

Optosensors based on membranes built of marine polysaccharides

Archana Johny

Master's Dissertation presented to
Faculty of Sciences of the University of Porto in
Chemistry-Specialization in Functional Materials
and Surfaces for Sustainability

2020

Advisor
Doctor Carlos Manuel de Melo Pereira,
Associate Professor,
Faculty of Sciences, University of Porto

Acknowledgement

“Gratitude is the fairest blossom which springs from the soul”

I take this opportunity to express my deep sense of gratitude to all those helped me to complete this project work successfully. First and foremost, I bow my head with infinite gratitude before Lord Almighty.

I owe my heartiest gratitude to my supervisor Prof. Carlos Manuel Melo Pereira and Prof. Manuel Azenha for their critical supervision, excellent guidance, and constant encouragement. Their insightful comments and openness during discussions truly helped me widen my perspectives in the research. Despite their busy schedules, they ensured 100% availability whenever I needed their help during this dissertation.

I express my deep sense of gratitude to Prof. Eduardo Marques, Master course director, for his constant support and encouragement throughout the study. I bestow my profound gratitude to the Erasmus Mundus SERP+ programme for giving me the opportunity to be part of the esteemed University of Porto. I am also deeply indebted to all my professors for giving me wonderful learning experiences.

I would like to express special thanks to my colleagues, Patrícia Santos and Cristina Queirós, who were always available to help me and give valuable suggestions throughout this study. I also thank all my lab members for providing me with a good working environment.

I am so thankful to my SERP+ colleagues and friends for making these two semesters full of joy and love.

I am deeply indebted to my beloved family for being the strongest pillar of support in all my decisions and constant encouragement to achieve my goals. I also thank Maria Jose who is no less than my family for making me feel home away from my home.

Finally, I would like to thank all those smiling faces in the Faculty of Sciences, U.Porto who have been very kind to me whenever in need of help, despite the language barrier.

Resumo

A toxicidade dos metais causa uma grande preocupação devido aos seus efeitos adversos nos sistemas vivos. Consequentemente, o desenvolvimento de sensores remotos, simples para detetar iões metálicos em amostras de água ganharam uma grande importância nas últimas décadas. Ao mesmo tempo, é importante focar os estudos no desenvolvimento de estratégias conducentes a uma economia circular e sustentável. O objetivo deste estudo é explorar potenciais aplicações de membranas, preparadas a partir de biopolímeros extraídos de resíduos marinhos, como sensores óticos para deteção de iões metálicos com toxicidade elevada.

Foram sintetizadas diferentes membranas usando quitosano e outros polissacarídeos de base marinha, como o sulfato de condroitina, fucoidano e ulvano, para o desenvolvimento de membranas sensoras, especificamente para deteção de alumínio (III). O cromóforo escolhido foi o Eriocromo de Cianina R, pois é conhecido por ter boa interação com Al (III) e ser capaz de dar um bom sinal devido à mudança de cor de amarelo para violeta após complexação com Al (III). O desempenho das membranas foi avaliado por espectroscopia UV-Vis. Foram estudados os efeitos do uso de tensioativos e diferentes métodos de sua incorporação na membrana. A adição de CTAB foi considerada benéfica para aumentar a sensibilidade das membranas do sensor. Este estudo também enfoca o efeito de iões interferentes na seletividade do sensor e na minimização do efeito destas interferências, especialmente a interferência causada pelo ião cobre nas membranas sensoras de Al (III).

Palavras-chave: Sensores; Membranas; Biopolímeros; Quitosano; Sulfato de condroitina; Fucoidano; Ulvano; Eriocromo Cianina R; Alumínio; Tensioativos; Interferência

Abstract

Metal toxicity is a major concern due to its adverse effects on living systems. Hence the development of simple remote sensors to detect metal ions in water samples have gained substantial demand in past few decades. At the same time, it is also important to focus studies on the development of strategies leading to a circular and sustainable economy.

The objective of this study is to explore potential applications of membranes, made of biopolymers extracted from marine wastes as optical sensors to detect metal ions.

Different membranes were synthesised using chitosan and other marine based polysaccharides such as chondroitin sulfate, fucoidan and ulvan for the development of sensor membranes, specifically to detect aluminium. The chromophore chosen was Eriochrome Cyanine R, since it has been known to have a good interaction with Al (III) and capable of giving a good signal due to its colour change from yellow to violet upon complexation with Al (III). The performance of the membranes was evaluated using UV-Vis spectroscopy. The effects of using surfactants and different methods of their incorporation into the membrane were studied. The addition of CTAB was found to be beneficial for enhancing the sensitivity of the sensor membranes. This study also focusses on the effect of interfering ions on the sensor selectivity and minimising their effect, especially the serious interference caused by copper to the developed Al (III) sensor membranes.

Keywords: Sensors; Membranes; Biopolymers; Chitosan; Chondroitin sulfate; Fucoidan; Ulvan; Eriochrome Cyanine R; Aluminium; Surfactants; Interference

Index

List of Figures and Tables

List of Abbreviations

ATR	Attenuated Total Reflectance
CAS	Chrome azurol S
CH	Chitosan
CS	Chondroitin Sulfate
CSB	Chondroitin Sulfate from Bovine cartilage
CTAB	Cetyl Trimethyl Ammonium Bromide
DTAB	Dodecyl Trimethyl Ammonium Bromide
ECR	Eriochrome Cyanine R
FTIR	Fourier Transform InfraRed spectroscopy
Fu	Fucoidan
GAG	Glycosaminoglycan
GalNAc	N-acetyl galactosamine
GlcA	Glucuronic acid
IR	Infrared
PCV	Pyrocatechol violet
TEOS	Tetraethyl orthosilicate
TIR	Total Internal Reflectance
Ul	Ulvans
UV-Vis	Ultraviolet - Visible
WHO	World Health Organisation

Chapter 1 – Introduction

1.1. Metal toxicity and importance of metal ion sensors

Metal toxicity is a major environmental issue posing threat to living systems. Metals, as chemical elements are ubiquitous, comprising almost 25% of earth's crust. Small doses of heavy metals like cobalt, copper, iron, manganese, molybdenum, vanadium, strontium, and zinc are essential requirements for living organisms. But the presence of excessive levels of essential metals and even small doses of toxic metals in the environment can influence both ecosystem and human health [1]. Consequently, they become capable of making alterations in the biochemical cycle which prove toxic to living organisms. Nonessential heavy metals like cadmium, chromium, mercury, lead, arsenic, and antimony can affect the surface water systems. They are transported by runoff water leading to contamination of water sources. All living organisms, plants, and animals depend on water for sustaining life. The intake of contaminated water thus transports toxic metal ions inside the cell, where they can undergo chemical changes causing severe health issues [2]. Hence the detection and monitoring of the presence of toxic metal ions in wastewater outlets, rivers, reservoirs, and other water sources hold high importance.

Powerful analytical techniques such as atomic absorption and emission spectroscopy, inductively coupled plasma mass spectroscopy, and their combination with chromatographic techniques are commercially available, which exhibit high sensitivity, selectivity, reliability, and accuracy. However, they require sophisticated instrumentation, complicated sample collection, pre-treatment, and a long measuring period, making it a non-viable choice for use outside the laboratory [3]. Hence there is high demand for simple, inexpensive, and portable instruments enabling real-time or even on-site analysis for monitoring the presence of environmental pollutants. Optical sensors are suitable candidates for such applications as they may easily be incorporated into low-cost, easy to use kits, yet at the same time, offering good selectivity and sensitivity necessary for environmental monitoring [4].

1.2. Optical sensors for the detection of metal ions

Sensors have attained substantial interest in past few decades as they are especially advantageous for *in situ*, and remote applications. A chemical sensor is a device that allows detection of one or more analytes and transforms chemical information into an analytically useful signal. Receptor and transducer are the two basic units of a sensor. Their main functions are recognition and transduction respectively. In the receptor part, the chemical information on recognition of analyte is transformed into a form of energy which may be measured by the transducer. Based on the receptor part, the sensor can be classified as:

- physical sensor, where no chemical reaction takes place;

- chemical sensor, in which a chemical reaction with the analyte gives rise to the signal;

- biochemical (biosensor), where a biochemical process is the source of the analytical signal.

Based on the operating principle of the transducer, chemical sensors can be classified as optical, electrochemical, electric, thermal, and piezoelectric sensors [5].

Optical chemical sensors have been investigated as viable alternatives to electrochemical sensors due to their lower detection limits and high sensitivity with no subjection to electrical noise. An optical sensor is a device capable of converting the changes in the properties of light like optical density into electronic signals. The device consists of four main components:

(a) Receptor where the identification of analyte takes place via specific interactions;

(b) Transducer that converts the recognition into optical signal;

(c) Light source which consist of at least one light emitting device;

(d) Detector which detects and converts the optical signal to suitable output.

The optical fibers have significantly contributed to the advancement in sensor technology. Transmission of light in optical fibres is based on the principle of total internal reflection (TIR). Sensors based on the fiber optics can be classified into two different categories: intrinsic sensors, where interaction with the analyte occurs within an element of the optical fiber; and extrinsic sensors, in which the optical fiber is used to couple light, usually to and from the region where the light beam is influenced [6]. In the case of intrinsic sensors, quantification is accomplished via measurement of absorption (ranging from the UV to the near infrared), or via luminescence. Spectrophotometric methods like UV-visible spectroscopy can be utilised in such cases, since they have advantages like accuracy, good precision, low cost, and simple operation. However optical ion sensing still has some limitations such as lack of specificity due to the interference with similar species having absorbance at the same wavelength [7].

1.3. Marine biopolymer membrane based optical sensors

Polymeric membranes are of great interest in scientific research for various applications. Due to relatively low cost and ability to tune the specificity by modifications, synthetic polymers have been dominating the sensing industry in past years. But natural polymers are gaining attention in recent times, as they can significantly contribute to the idea of shifting to a circular economy, which is a need of the hour. This study focuses on sensor membranes made up of natural polymers such as chitosan, chondroitin sulphate, fucoidan, ulvan etc extracted from marine wastes. The use of such biodegradable polymers is on demand due to its biocompatibility, availability, and low cost [8]. The polymers that make up the membrane provide a solid support for the immobilisation of chromophores. Moreover, they also play a significant role in enhancing the selectivity and permeability of the species that interact with the analyte.

1.3.1. Chitosan

Chitosan (CH) is one of the most important biopolymers that is widely being used in various applications due its non-toxic, biocompatible, and biodegradable nature [9]. Chitosan is generally found in nature as a macromolecular compound called chitin, which is a natural polysaccharide. This biopolymer is extracted from marine organisms and is a major constituent of shrimp and crab shells. Chitin consists of repeating units of N-acetyl-D-glucosamine and deacetylation of chitin leads to formation of chitosan. The deacetylation process of chitin leads to formation of amine groups. It is also interesting to find that their molecular structure has similarity to that of cellulose. The chemical structures of chitosan and chitin are like cellulose except that C-2 position hydroxyl group of cellulose is replaced by acetyl group in chitin and amino group in chitosan [10]. The structure of Chitin and Chitosan is given in Figure 1.

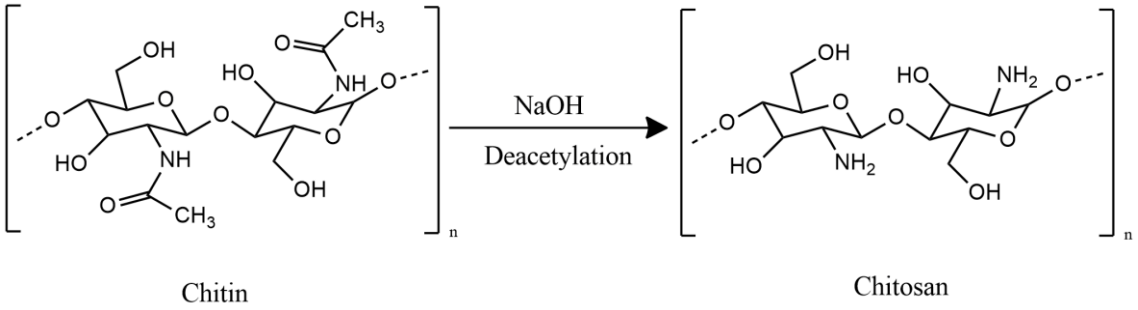

Fig. 1 - Deacetylation reaction of Chitin to give Chitosan

Chitosan is more efficient than chitin in adsorption capacity due to the presence of amino groups on polymer chains. It has a pKa value of around 6.5 and thus at lower pH (<6.5), the amines will be protonated and acquire positive charge, rendering polycationic behaviour to chitosan. At high pH (>6.5), de-protonation of amine groups occurs causing chitosan to lose charge and become insoluble. The properties of chitosan depend on its molecular weight and degree of deacetylation. Chitosan, due to its polycationic property, can be used with metal anions, dyes, etc. to improve coagulation and as a filtration membrane for the removal of contaminants from water [11], [12]. Another fascinating aspect of chitosan is its ability to form films and membranes, with selective permeability

and good mechanical properties. This can be attributed to the large number of amine and hydroxyl functional groups, resulting in stronger inter and intramolecular hydrogen bonds [13].

Chitosan is insoluble in water and dissolves in weak acids. The type of acid used for dissolution also influences the mechanical properties of films. Chitosan dissolved in acetic acid solution forms dimers, which indicates relatively strong intermolecular interaction. Chitosan films casted using acetic acid as solvent tend to have greater tensile strength than those from other acid solutions [13]. The mechanical properties of the film can also be altered by the changing the degree of deacetylation, molecular weight, pH, and type of solvent used [14].

Chitosan has been extensively used for various applications [15] as illustrated in the Figure 2.

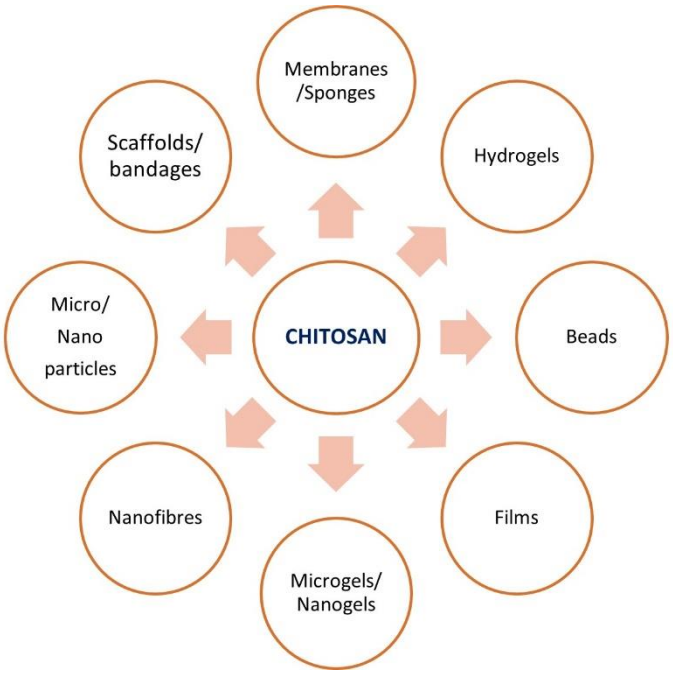

Fig.2 - Schematic representation of processing chitosan into various forms and applications. Figure adapted from [15]

1.3.2. Chondroitin sulfate

Chondroitin sulfate (CS) is a glycosaminoglycan (GAG), a water soluble heteropolysaccharide composed of repeating disaccharide units comprising an amino sugar (N-acetyl galactosamine, GalNAc) and glucuronic acid (GlcA) linked by β-(1 → 3) glycosidic bonds [16]. The position of sulfate group is the major defining factor for classification of CS types: carbon 4 (CS-A), 6 (CS-C, more common), both 4 and 6 (CS-E), positions 6 of GalNAc and 2 of GlcA (CS-D) and 4 of GalNAc and 2 of GlcA (CS-B) [17]. The corresponding structures are depicted in Figure 3.

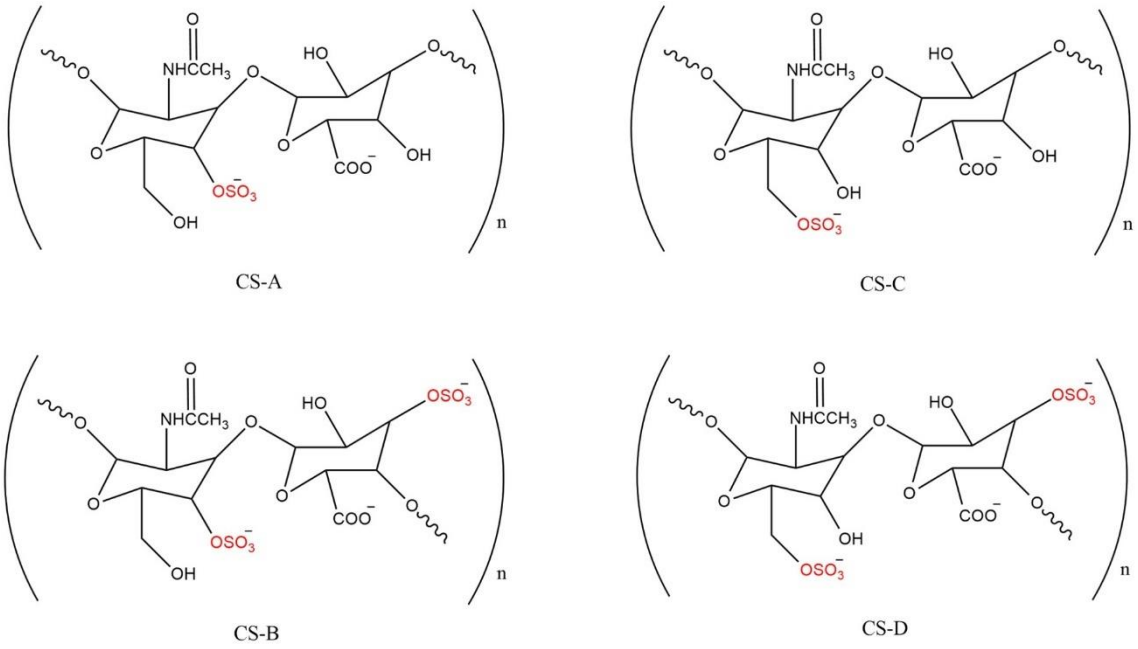

Fig.3 - Schematic representation for structures of different types of Chondroitin sulfate

GAGs are obtained from mammalian tissues mainly generated in slaughterhouses: rooster combs, cartilage (tracheas and nasal from bovine and swine) and umbilical cords [18]. CS is a linear anionic polysaccharide present in cartilage, bone, and connective tissue. The presence of the -O-SO_3^- groups in the structure of CS provides them permanent negatively charged points even at low pH values. The cooperativity between sulfate and other nearby functionalities attached to the backbone of the biopolymers

(COOH/COO^-, OH and $NHCOCH_3$) envisage strong binding towards cationic species [16]. The crosslinking of CS via the sol-gel reaction can give a rigid microporous biopolymer-silica composite, maintaining the original ability of CS to complex metal cations via the carboxylate and sulfonate groups. This allows the exploitation of the negatively charged CS for metal cation related applications such as opto-sensitive sensor preparations [19]. The combination of CH and CS can be explored for great potential applications since it enhances hydrophilicity, biological compatibility, mechanical strength [20].

1.3.3. Fucoidan

Fucoidan (Fu) is an anionic polysaccharide extracted from brown seaweeds and some marine invertebrates (such as sea urchins and sea cucumbers). The polysaccharide was first isolated from marine brown algae by Kylin in 1913 [21]. Fucoidans are primarily composed of L-fucopyranose units and sulfated ester groups. They could also contain some other monosaccharide units including mannose, glucose, galactose, and xylose connected randomly within the polymer network with randomized sulfate group substitutions [22].

Fucoidan has a brownish powder appearance and it disperses easily in water. Due to the high dielectric constant of water, oppositely charged groups are shielded, and they are surrounded by hydration shells. If solvents like ethanol are used, because of its lower dielectric constant, the sulfate ester and positive ions can form ionic bonds, which results in precipitation [23].

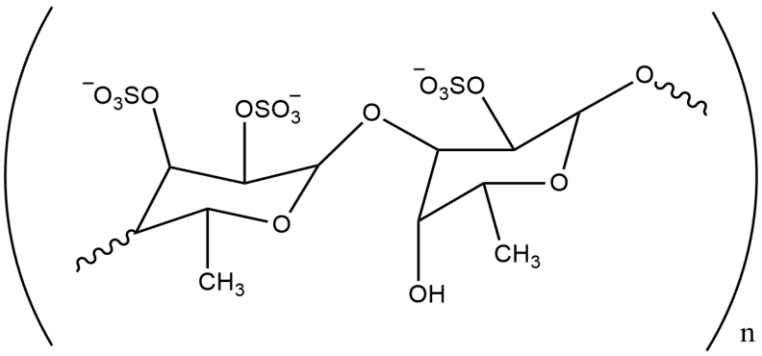

Fig.4 - Structure of Fucoidan

Fucoidan can form polyelectrolyte complexes with chitosan [24] due to the presence of sulfate groups, which as in CS allows interaction with metal ions. Because of the sulfate ester groups, which are linked to the carbohydrate backbone, fucoidans exhibit high anionic charges even at low pH values [23]. This property makes fucoidan an interesting candidate for the membrane fabrication via sol-gel crosslinking for sensor applications.

1.3.4. Ulvans

Ulvans (Ul) are a rather unexplored group of anionic polysaccharides with great versatility and potential. They are extracted from the cell-walls of green seaweeds *(Ulva lactuca)* [25]. Ulvans are water soluble and semi crystalline in nature. Sulfated rhamnose, xylose, glucuronic and iduronic acids are the main constituents of ulvan [26]. The structure of Ulvans is shown in Figure 5.

Ulvan has been reported as an anticoagulant, antioxidant, antitumor and immune modulator [27]. The significant biological activities of ulvan, in combination with its tunable physicochemical and rheological properties have triggered high interest for its utilization in hybrid biomaterials [28]. A recent study showed that ulvan polysaccharide-based films have good optical, barrier, and antioxidant properties [29]. This study will explore the use of ulvan for fabrication of membranes for optical sensing applications.

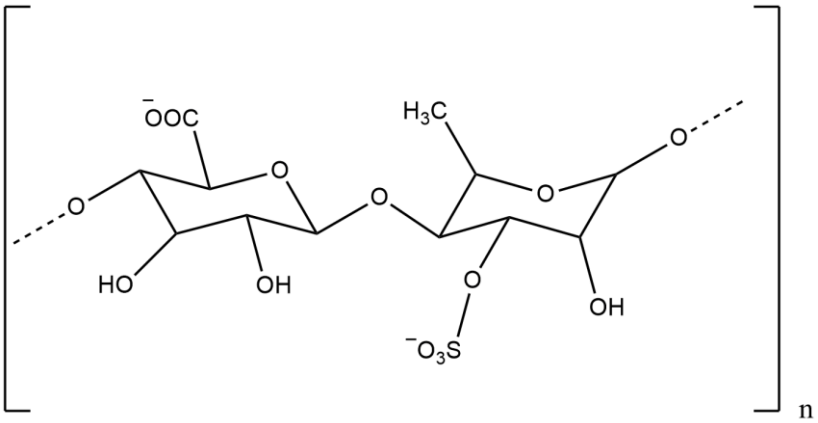

Fig.5 - Structure of Ulvan

Anionic ulvan and cationic chitosan, two; polymers with oppositely charged backbones, can be combined to form novel supramolecular structures of stabilized membranes through electrostatic interactions [25]. This can be assisted with the sol-gel process to form sensitive membranes with specificity for certain metal ions on immobilisation using chromophores. Considering its natural availability with minimal concerns regarding toxicity towards host organisms as well as the ease of functionalization of its hydroxyl and carboxyl groups, ulvan can be considered as a versatile functional material for tailor-made applications.

1.3.5. Sol-gel process

The sol-gel process is a wet-chemical technique. In general, the sol-gel process can be regarded as the preparation of the sol, gelation of the sol and removal of the solvent. The overall sol-gel process can be represented by the following sequence of transformations [30]:

Silicon alkoxides are the typical precursors used for the preparation of gels and a typical example is tetraethyl orthosilicate (TEOS).

In the sol-gel process, a sol of a given precursor is prepared, which involves the dissolution of the alkoxides in a suitable solvent (commonly alcohol), which undergo hydrolysis, followed by polycondensation reactions to produce highly condensed and branched networks, the gel.

Generally, three reactions are used to describe the sol-gel process: hydrolysis, alcohol condensation and water condensation. Because water and alkoxides are immiscible, alcohol is commonly used as co-solvent. Due to the presence of the co-solvent, the sol-gel precursor, alkoxide, mixes well with water to facilitate the hydrolysis. The hydrolysis reaction is usually either acid or base catalysed.

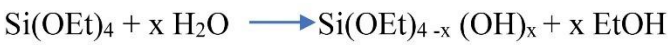

…….. Eq.1

The hydrolysed or partially hydrolysed molecules may link together. This condensation reaction produces either water, called water condensation;

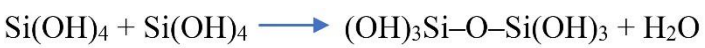

…….. Eq. 2

or ethanol, called alcohol condensation.

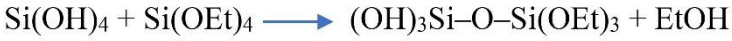

…….. Eq.3

Combination of above three reactions leads to the formation of silicon dioxide by the following reaction:

…….. Eq. 4

The sol gel process thus provides matrices for the biopolymer membranes. Hence the process has gained particular interest in fabrication of membranes used as optical sensors for the detection of analytes like heavy metal ions. Since they have no absorption in the near UV and visible, sol-gels are well suited for fabrication of dyed materials in the form of films, fibers, etc [7].

In this study, some components other than biopolymer and sol gel process constituents have been used for the fabrication of membranes to obtain desired properties. Plasticizers and crosslinking agents are two very important components required for obtaining membranes with integrity and malleability. Glycerol is a known plasticizing agent for biopolymers with the ability to improve the flexibility of films prepared. Similarly, glutaraldehyde was employed as the crosslinking agent in the synthesis methodology to improve the mechanical property of the membrane formed.

1.4. Optical Sensor for the detection of Al (III) ions

Aluminium is the third most abundant metal found in earth's crust. It has many applications in various industries such as textile, paper, cosmetics, pharmaceutical, etc. However, aluminium has no biological role and is a toxic nonessential metal to microorganisms. According to a WHO report, the average daily intake of aluminium by humans is approx. 3-10 mg [31]. It has been reported that the metabolic pathways involving calcium, phosphorus, fluorine, and iron metabolism are adversely affected by aluminium in the living organisms. In humans Mg^{2+} and Fe^{3+} are replaced by Al^{3+}, leading to various disturbances associated with intercellular communication, cellular growth, and secretory functions. Al^{3+} have reported to have a verified role in Parkinson's disease and Alzheimer disease. The decrease in pH of soil and water caused by acid rain can trigger an increase in aluminium toxicity which in turn results in the drying of forests, plant poisoning, crop decline or failure, and death of aquatic animals [32].

The main objective of this dissertation is to design and develop a suitable optical sensor based on marine biopolymers for detection of Al (III) ions, by the immobilisation of a suitable chromophore. According to the literature, the most commonly used chromophores for the determination of aluminium were found to be chrome azurol S (CAS), pyrocatechol violet (PCV) and Eriochrome Cyanine R (ECR) [33]. It was found that Eriochrome Cyanine R is a good chelating agent for binding aluminium forming stable ECR-Al (III) complexes [34]. ECR is a well-known reagent for the trace determination of aluminium that forms a 3:1 complex at higher concentrations and 2:1 or 1:1 complex at lower concentrations of the reagent. It was found that the formation of the ECR-Al (III) complex is maximum in the acidic to the natural pH range (pH 5-6) [4]. ECR is soluble in water due to a sulfonic group in its chemical structure as given in Figure 6.

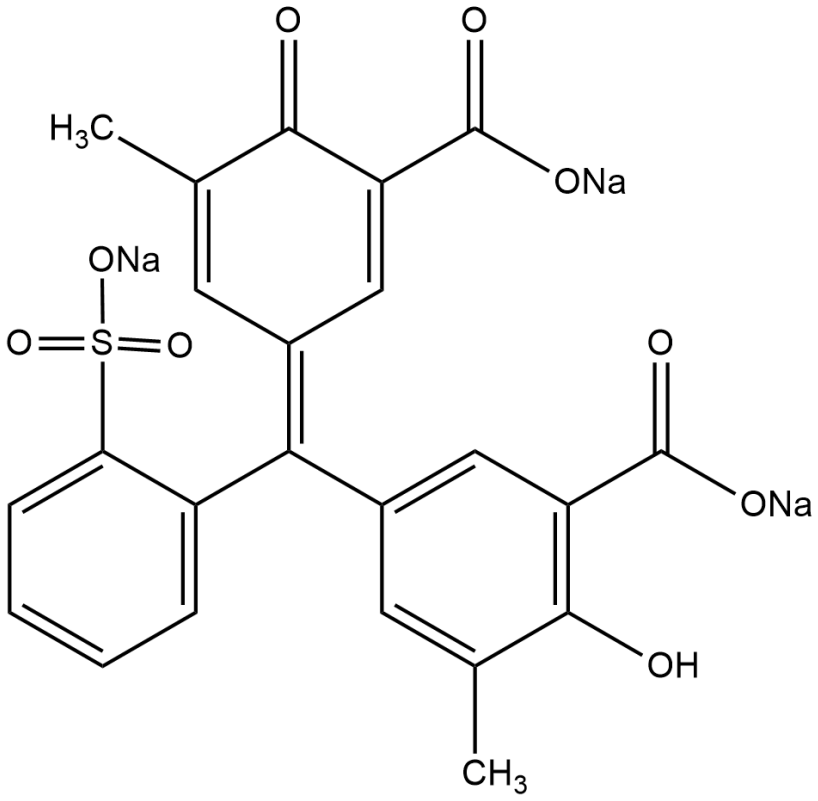

Fig.6 - Structure of Eriochrome Cyanine-R

Chapter 2 – Instrumentation Techniques

2.1. Attenuated Total Reflectance - Fourier Transform InfraRed (ATR-FTIR) spectroscopy

ATR-FTIR spectroscopy is an important analytical tool for probing the local surface structure of a material, allowing the study of the composition and chemical modifications made on the surface. The penetration depth of infrared (IR) light in the sample for ATR measurements is independent of sample thickness [35].

In IR spectroscopy, a sample is illuminated with a monochromatic light source. Absorption will occur if the frequency of light corresponds to the vibrational frequency of the bond; this is then apparent in the spectrum of transmittance and can be correlated to how much energy has been absorbed. FTIR has a much faster sampling time and higher signal to noise ratio. In FTIR, a broadband/polychromatic light source is used to illuminate the source. The beam first passes through a Michelson interferometer, a beam splitting device which causes a deliberate path length shift or retardation, subsequently illuminating the detector after hitting the sample with a mixed interference beam of all wavelengths. The detector produces an interferogram, a fixed set of retardation values and a corresponding set of intensities. The resultant FTIR spectrum is a set of inverse lengths (cm^{-1}) versus intensity. Bonds can thus be assigned to intensities at certain wavenumbers.

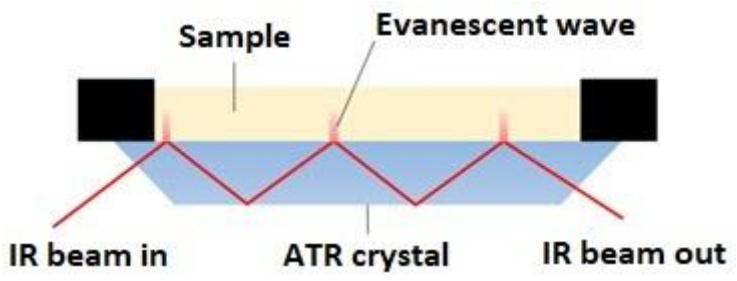

Fig.7 - Schematic illustration of a working ATR crystal in an ATR-FTIR spectrometer

A solid or liquid can simply be placed on the ATR crystal with a small amount of pressure to form an intimate contact, and then analysed. Compared to traditional FTIR methods, which rely on transmission and therefore a diluted sample/thin film, ATR-FTIR relies on Total Internal Reflectance (TIR) and thus does not have this issue. The sample is also then reusable, and uncontaminated. The beam of infrared light is incident on the ATR crystal, passing through and reflecting off the sample (Figure 7). As a result of TIR, an evanescent wave is set up, propagating through the crystal, and reflecting of both crystal and sample consecutively [36].

2.2. Ultraviolet - Visible Spectroscopy

Optical sensors coupled with UV visible detectors is a powerful tool for monitoring heavy metals in aqueous medium. The development of optical fibre probes allowed easy implementation of spectroscopic methods to real time monitoring.

Typically, a spectrophotometer uses a tungsten light source for the near-UV to near IR spectral range (e.g. 380–1000 nm) and a deuterium discharge lamp for the UV from about 200 to 380 nm. Monochromator produces monochromatic light by removing unwanted wavelengths from the source light beam. A UV-Vis spectrometer can be either single beam or double beam. In a single beam instrument, all the light passes through the sample cell. Intensity of incident light (I_o) must be measured by removing the sample. In other words, baseline measurement should be carried out prior to sample analysis. The double beam instrument has a reference cell and sample cell, and the analysis is always performed simultaneously. Finally, the light after passing through the sample/reference reaches the detector giving corresponding output data.

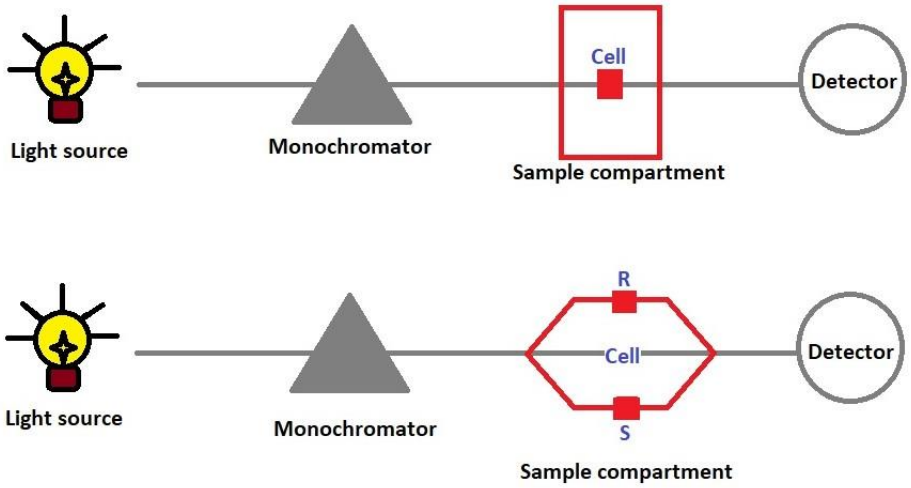

Fig.8 - Schematic illustration of a single beam (top) and double beam (bottom) UV-Vis

Typically, in a UV-Vis spectroscopy measurement, a beam of light of intensity I0 interacts with the analyte and the transmitted light is collected by a detector. The transmittance T of the sample is defined as the ratio of the intensities of transmitted light (I) over incident light (I_o). The fraction of light absorbed is reported in terms of absorbance A(λ), defined as

$$A = -\log T \qquad \text{..... Eq.5}$$

Thus, basically absorbance and transmittance provide the same information. Usually, the former is used since the relationship between absorbance and both concentration and path length are linear. The absorbed radiation follows the Lambert Beer law [37].

$$A(\lambda) = C\varepsilon l \qquad \text{..... Eq.6}$$

C is the concentration of the analyte, l is the path length of the cell and ε is the molar extinction coefficient, given as a function of the wavelength and expressed in L mol^{-1} cm^{-1} , which is an intrinsic property of chemical species that gives information on how strongly light at a given wavelength is absorbed.

Chapter 3 – Experimental Procedures

3.1. Materials and reagents

Ulvan, extracted from *Ulva lactuca* was kindly provided by Stemmaters, Portugal. Chondroitin sulfate sodium salt, extracted from bovine cartilage was provided by Carbosynth, UK and Fucoidan extracted from *Fucus vesiculosus* was provided by Marinova, Australia. Chitosan, glutaraldehyde, acetic acid, and sodium acetate were purchased from Sigma Aldrich, Germany. Metal cation salts such as lead nitrate, cadmium nitrate, copper sulphate, sodium fluoride, and ferrous sulphate were supplied by Merck, Germany. Hydrochloric acid, anhydrous glycerol, aluminium sulphate hexadecahydrate, and ammonium dichromate were purchased from Fluka, Switzerland while eriochrome cyanine R and ferric sulphate were purchased from Riedel-de Haen, Germany. Nitric acid and cetyl trimethyl ammonium bromide were purchased from PanReac, Spain and dodecyl trimethyl ammonium bromide from Sigma Life Science, USA. Tetraethylorthosilicate was purchased from Acros organics, Germany and absolute ethanol was from Fischer Scientific, UK. Water used was of Milli-Q purity, Millipore, Italy.

3.2. Instrumentation

Attenuated total reflectance - Fourier Transform Infrared Spectroscopy (ATR-FTIR) measurements were performed in the range of 600 – 4000 cm^{-1} using spectrophotometer Bruker FT-IR System Tensor 27 with diamond ATR crystal. The pH of the buffer solution was adjusted using Metrohm 691 pH Meter. PG instruments UV-Vis spectrophotometer, T60, was used to record the absorption spectrum of the membrane analysed.

3.3. Procedures

3.3.1. Synthesis of the membranes

Here, we present the preparation of the four types of the four types of chitosan-based sol gel membranes. The procedure followed for the synthesis of membranes was primarily adapted from the one described in the literature [38] with necessary modifications in accordance with the type of membranes prepared. The initial step of preparation of the TEOS solution is the same for all the membranes and is a major step for the formation and incorporation of silica by the sol-gel process. For this a solution containing 5.5 mL of TEOS, 5.5 mL of ethanol, 22.2 mL of deionized water and 1.25 mL of 0.1 mol/L HCl was prepared and left under moderate magnetic stirring for a period of 24 hours.

3.3.1.1. Synthesis of Chitosan (CH) membranes

The CH solution of a concentration of 3% (m/v) was prepared by dissolving in 2% acetic acid solution. 10 mL of 3% CH solution was mixed with 5 mL of already prepared TEOS solution and allowed to stir for 2 hours. The next step consisted of the addition of 2 mL of 8% (m/v) glycerol, which acts as a plasticizer and the solution was kept under stirring for another 2 hours. This was followed by the addition of 150 µL of 2.5% (m/v) glutaraldehyde, a cross-linking agent. After stirring for 1 hour, 8 mL of the final solution was deposited into a Petri dish of about 80 mm in diameter and allowed to dry at room temperature. Once dried, the desired membrane obtained is removed from the Petri dish and stored in airtight plastic containers.

3.3.1.2. Synthesis of modified Chitosan membranes

Three different types of membranes were synthesised by mixing chitosan with containing Chondroitin Sulfate from Bovine cartilage (CH-CSB), Fucoidan (CH-Fu) and Ulvans (CH-Ul). This modified synthesis consisted of the preparation of two initial solutions, which

would later be added to each other. Firstly, 9 mL of 3% (w/v) CH in 2% acetic acid solution was prepared. Secondly, 9 mL of 0.2% (w/v) polysaccharide (CSB or Fu or UI) in aqueous solution was prepared, depending on the type of membrane to be synthesised. These two solutions were mixed and kept under magnetic stirring for about 2 hours. Then 4.5 mL of already prepared TEOS solution was added to it and allowed to stir for 2 hours. The next step was the addition of 3 mL of 8% (m/v) glycerol, which after 2 hrs of stirring was followed by subsequent addition of 225 µL of 2.5% (m/v) glutaraldehyde. After stirring for 1 hour, 10 mL of the final solution was deposited into a Petri dish of about 80 mm in diameter and allowed to dry at room temperature. Figure 9 shows the schematic representation of the procedure for the synthesis of the membrane.

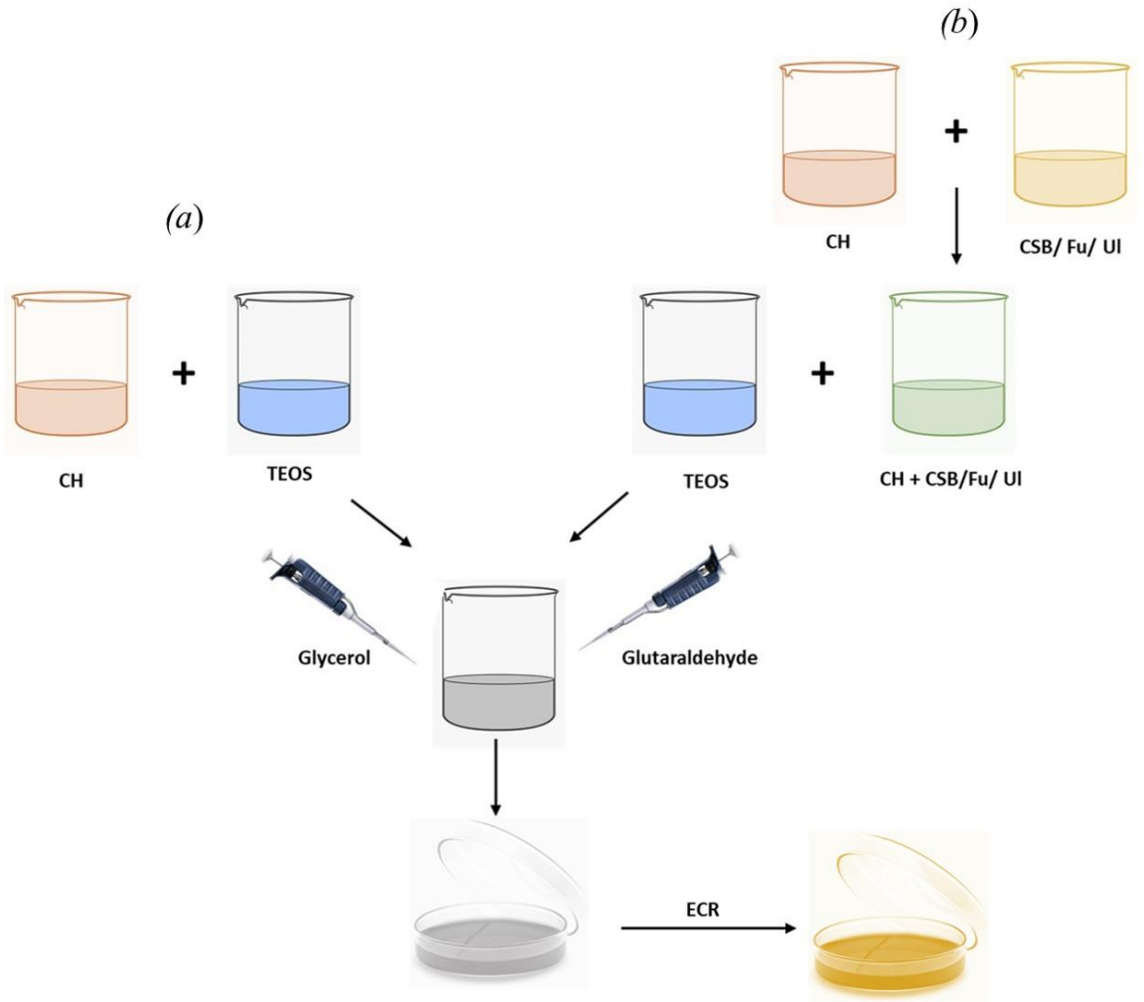

Fig.9 - Schematic representation of the synthesis of sensor membrane (a) simplest synthesis method of CH membrane (b) modified synthesis method of CH membranes containing CSB/Fu/UI

3.3.2. Development of sensor membranes for Al (III) ions

The immobilisation of a suitable chromophore into the analysing membrane is a crucial step in the fabrication of sensor membranes. In this study, eriochrome cyanine-R (ECR) has been chosen to be the chromophore for developing sensor membranes for Al (III) ions. 0.25 mmol/L ECR solution was prepared using millipore ultrapure water. 150 mg of the membrane to be analysed was weighed to immerse in 10 mL of ECR solution for 24 hours for successful incorporation of ECR into the membrane. Then it was washed using ultrapure water for further analysis.

3.3.3. Evaluation of sensor membranes for Al (III) ions

Before evaluation of the developed sensor membranes, it was necessary to prepare some solutions.

3.3.3.1. Preparation of the buffer solution

Buffer solution of sodium acetate / acetic acid of concentration 0.002 mol/L was prepared at pH 5. For its preparation, 0.1041 g sodium acetate salt was dissolved in 1 L of solution. 0.0417 mL of acetic acid was added, the pH being adjusted with 5% HNO_3.

3.3.3.2. Preparation of Aluminium ion Solutions

Metal cation solutions were prepared from the aluminium sulphate salt [Al $(SO_4)_3$]. The salt was dissolved in 0.002 mol/L acetate / acetic acid buffer at pH 5. A 100 mg/L of Al (III) solution was prepared, from which a set of desired concentrations (1 to 20 mg/L) was obtained by dilution. These solutions needed to be prepared on each day of analysis, due to the possible instability of the metal cations in this buffer.

3.3.3.3. Optimization of immersion time in metal ion solutions

The immersion time of ECR incorporated membranes in metal ion solution was optimized by immersing them in a 10 mg/L solution of aluminium cation. The immersion time varied

from 1 to 40 min. The sensor membrane was subjected to immediate analysis by UV-Vis spectroscopy, in the range from 380 to 700 nm.

3.3.3.4. Sensor calibration

After preparation of the optimized sensor membrane, it was analyzed in UV-Vis spectrophotometer. The ECR incorporated membrane, before immersion in the metal ion solution was used as blank for the spectrophotometric readings in the range of 380 to 700 nm. The membrane is then immersed in an acetate buffer solution of pH 5 for 32 min and absorbance was measured. Subsequently, the same membrane was subjected to immersion in different concentrations of metal ions solution (from 1 to 20 mg/L) prepared in acetate buffer of same pH for regular intervals of 32 min and absorbance was measured for each case. From the spectral data obtained, the change in absorbances were calculated with respect to the conditioning buffer solution, i.e., as $\Delta A = A - A_0$, where A and A_0 are the absorbances of the sensor in Al (III) solution and buffer solution alone, respectively. The UV-Vis spectra obtained were analyzed using the OriginPro9 program. Peaks and baseline analysis were carried out as represented in Figure 10 to find the absorbance maxima and corresponding wavelength.

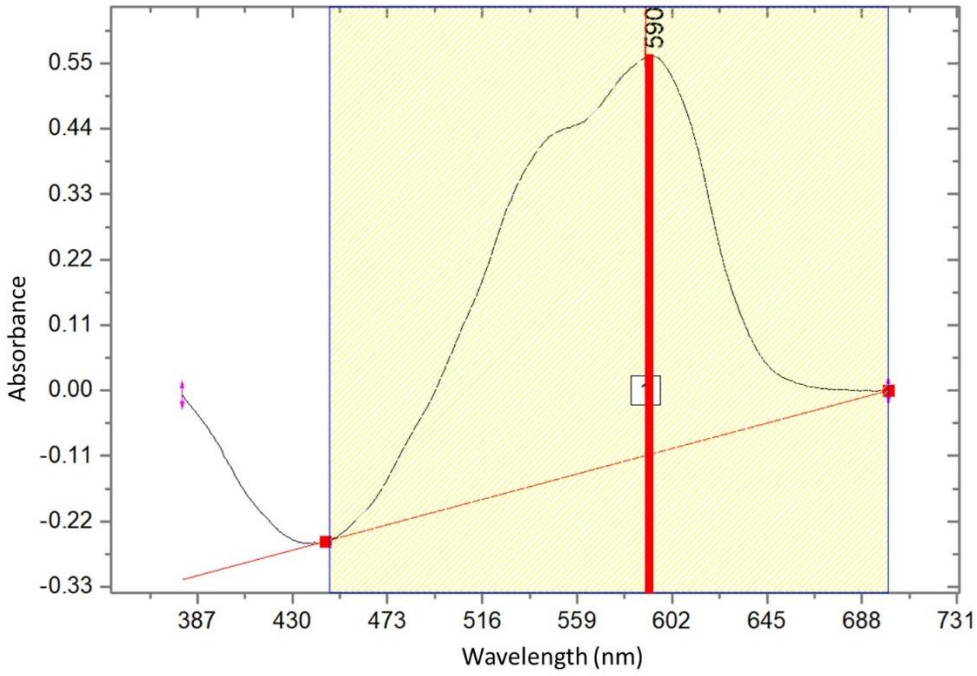

Fig.10 - Example of the method used to determine the height of the peak at 590 nm

3.3.3.5. Study of the effect of surfactants

The incorporation of surfactants into the membrane is expected to enhance the optical performance of the sensor membranes. For this, two methods of incorporation of the cationic surfactants (cetyl trimethyl ammonium bromide, CTAB and dodecyl trimethyl ammonium bromide, DTAB) were carried out and analyzed in this study. The first method was an approach to incorporate the surfactants into the membrane during the synthesis. The procedure of synthesis is almost like the one described in 3.3.1.2. The only difference is that, depending on the type of membrane prepared, 9 mL of 0.2% CSB or Fu or Ul solution also contained the surfactant (CTAB or DTAB) in two different ratios (1:1 and 1:2 ECR-surfactant). This solution was added to 3% chitosan solution and stirred for 2 hours. Subsequently TEOS solution, glycerol and glutaraldehyde were added each after 2 hours of stirring and the CTAB incorporated membrane is casted by depositing 10 mL of the final solution into a Petri dish having 80 mm diameter. Figure 11 depicts the experimental procedure for the first method used for the analysis.

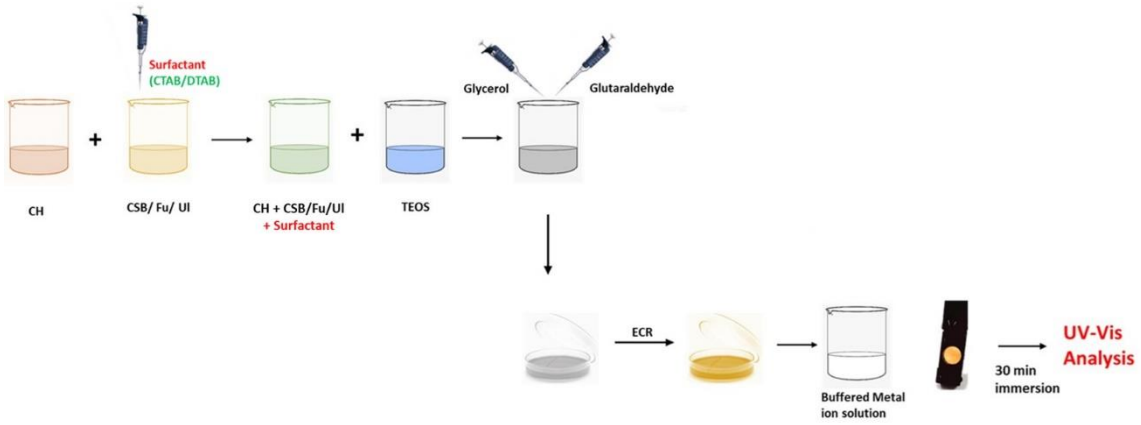

Fig.11 - Schematic representation of the procedure followed to incorporate CTAB into the membrane, during the synthesis

The second method was an approach to incorporate the surfactant into the membrane after the synthesis. The procedure for the synthesis of the membrane is the same as explained in 3.3.1.2. The membrane is prepared by casting the solution containing chitosan, CSB or Fu or Ul, TEOS, glycerol and glutaraldehyde. The synthesized

membrane was subjected to ECR incorporation. In this method, the surfactant is incorporated during the final step where, the sensor membrane is immersed in the analyte sample solution, which also contained appropriate volume (0.5 mL or 2 mL) of 1 mmol/L surfactant along with 10 ml of the metal cation solution in acetate buffer of pH 5. Figure 12 depicts the experimental procedure for the second method.

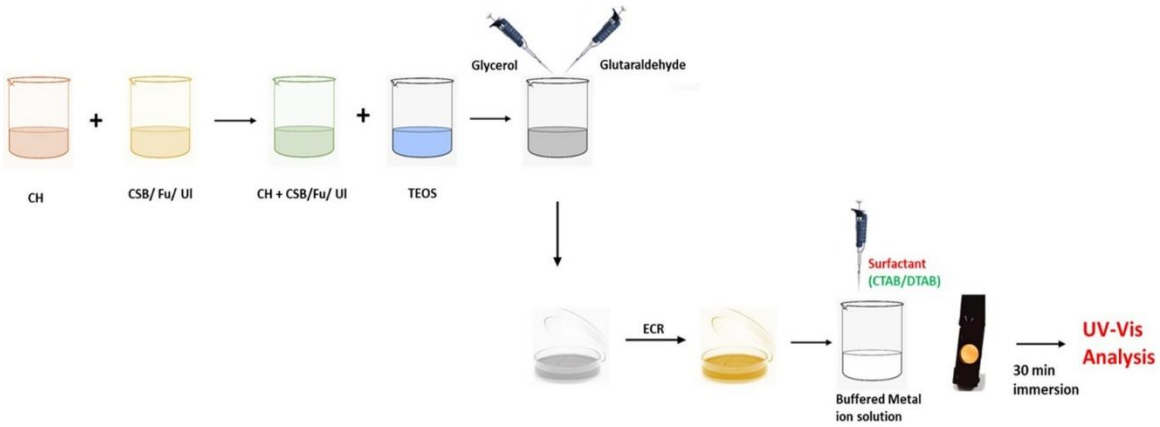

Fig.12 - Schematic representation of the procedure followed to incorporate CTAB into the membrane, after the synthesis

3.3.3.6. Study of the effect of interfering species

The potential interfering ions to Al (III) like Cu (II), Fe (II), Fe(III), Cd (II), Pb (II), Cr (VI) and F^- were selected for analysis to study the effect of interfering species. In the initial study, the membranes were analysed using UV-Vis spectroscopy by immersion in different concentrations of corresponding metal ion solutions for 32 min, to identify the interfering ions. The influence of the identified interfering species was studied by immersing the membrane in a solution containing fixed concentration of Al (III) ions along with varying concentrations of interfering ions. After immersion for 32 min, UV-Vis analysis was carried out. From the data obtained, selectivity coefficient was calculated. The influence of incorporation of CTAB to CSB membranes in the effect of interference was also studied.

Chapter 4 – Results and Discussions

4.1. Membrane composition assessment using ATR-FTIR spectroscopy

The composition of the prepared membranes was analysed using Fourier Transform Infrared Spectroscopy coupled with attenuated total reflectance (ATR) module. For confirming the presence of expected components, FTIR spectra of CH, Ul, Fu and CSB samples were studied for reference. Figure 13 illustrates the FTIR spectra of the individual components namely, CH, Ul, Fu, and CSB, respectively.

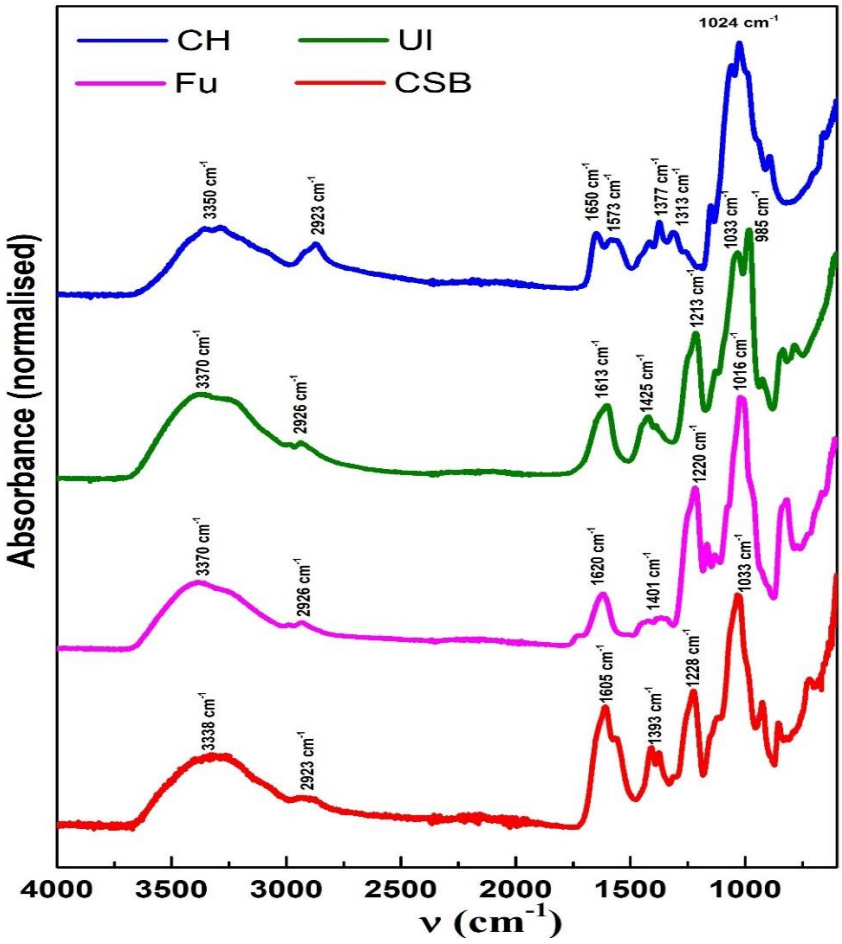

Fig.13 - FTIR spectra of components CH, Ul, Fu and CSB in powder form

As indicated in Figure 13, the broad bands in the range of 3200-3500 cm^{-1} due to vibrations of O-H bonds and C-H stretching bands around 2926 cm^{-1} are common in all the four spectra [39]. Chitosan shows two characteristic bands at 1650 cm^{-1} and 1573 cm^{-1} indicating C=O stretching band of the acetyl group (amide I) and -NH bending and stretching (amide II) bands respectively [40]. However, the stretching vibrations of S–O bonds at 1220 cm^{-1} and the carboxylic peaks at about 1620 cm^{-1} and 1400 cm^{-1} are typical for sulfated polysaccharides like CSB, Fu and Ul [41]. In addition, the bands at 1016 cm^{-1} to 1033 cm^{-1} indicates C–O–C stretching vibrations and bands around 980 cm^{-1} represent asymmetrical stretching vibration of C-O-S bonds, while the signals in the range of 822 cm^{-1} and 849 cm^{-1} were assigned to the symmetrical stretching vibrations of C-O-S bonds [42].

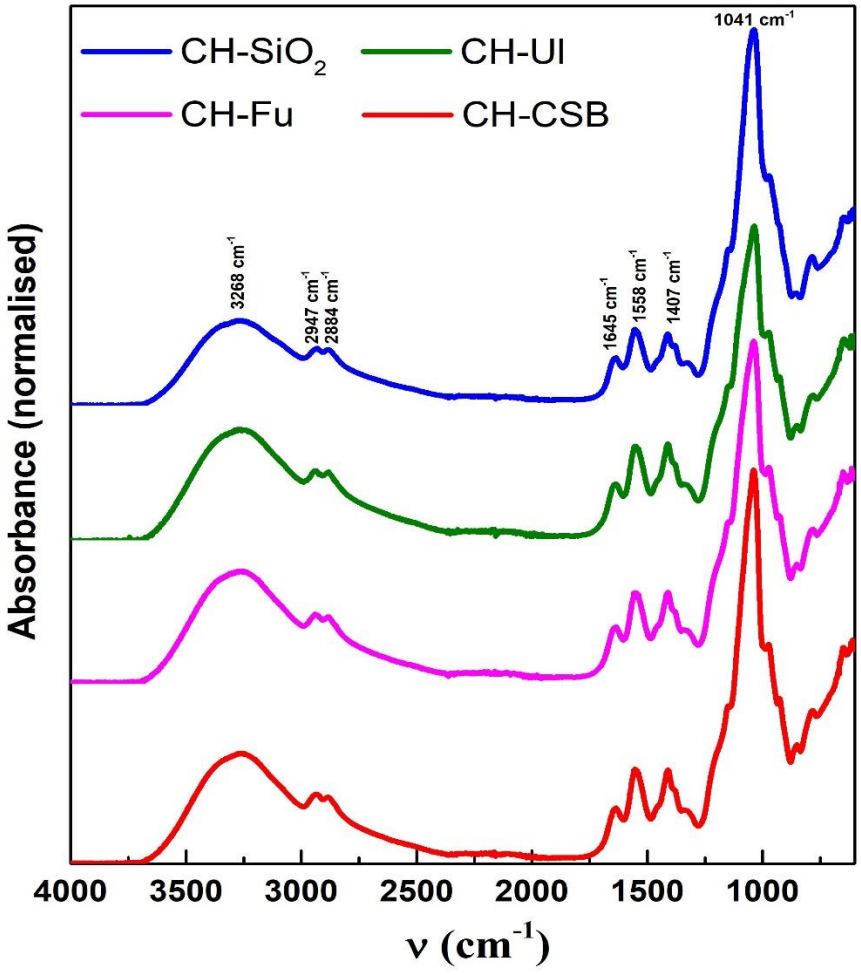

Fig.14 - FTIR of the different types of membranes

The FTIR spectra of the different types of chitosan-based membranes (Figure 14) also give similar characteristic peaks relative to individual compounds. It is possible to verify the presence of silica from the peaks at 1041 cm^{-1}. In addition, the appearance of characteristic peaks at 1558 cm^{-1} and 1645 cm^{-1} mark the presence of chitosan in the CH-Ul, CH-Fu and CH-CSB membranes. However, unequivocal identification of Ul, Fu and CSB membranes is not possible because of the overlapping of absorption bands as their theoretical mass percentage gets reduced relative to that of other constituents, causing low intensity bands.

4.2. Development of sensor membranes for the detection of Al (III)

The successful incorporation of a chromophore into the membrane is a crucial step in obtaining a sensor membrane. A suitable chromophore on complexation with the analyte metal ion can produce a colour change, and hence the presence of analyte can be verified by optical measurements [43]. Al (III) ions, being the metal cation of interest in this case, Eriochrome Cyanine R was chosen to be the suitable chromophore. The optimized concentration of ECR used in this study was 0.25 mmol/L.

Two methods were studied for the incorporation of ECR into the membrane. The first method studied was the incorporation of ECR during the synthesis. The expected outcome was to obtain ready to analyse, homogeneously coloured sensor membrane. However, when prepared, it was observed that the corresponding solution containing ECR, gradually lost its colour upon the addition of 2.5% glutaraldehyde, prior to membrane casting as given in Figure 15. The transparent membranes obtained via this method failed to produce any colour change when immersed in 20 mg/L Al (III) solution.

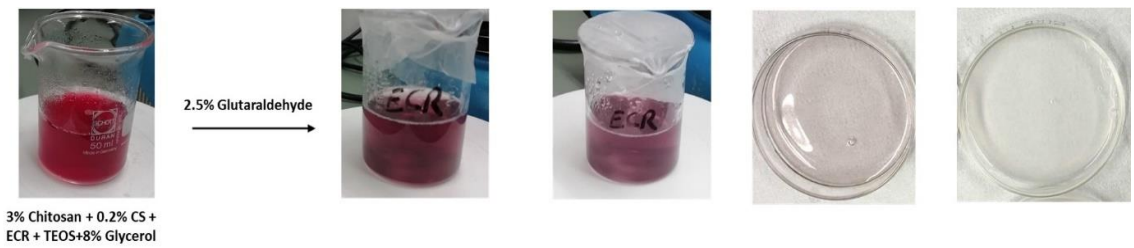

Fig.15 - Changes in ECR colour upon addition of glutaraldehyde

Various methods were tried to resolve this problem like addition of lower percentage of glutaraldehyde and different pH conditions, but no good results were obtained. It was found that the addition of nitric acid after the glutaraldehyde addition step could regenerate the lost colour of the membrane (Figure 16). Hence, the effect of adding different acids like 2% (v/v) HNO_3, 2% (v/v) CH_3COOH, and 2% (v/v) H_2SO_4 was studied. Both sulfuric acid and nitric acid were able to regenerate the lost colour of ECR in the solution. This effect was produced due to the extreme acidic conditions (pH=0) created upon addition of strong acids and acetic acid being a weak acid could not reproduce the effect. However, the membranes so obtained were not good enough in terms of selectivity and stability. The colour change produced in the presence of Al (III) faded within 10 minutes. Also, the membranes showed colour change even with buffer solution and water. Hence, we had to find an alternate method of ECR incorporation into the membrane to get the desired results.

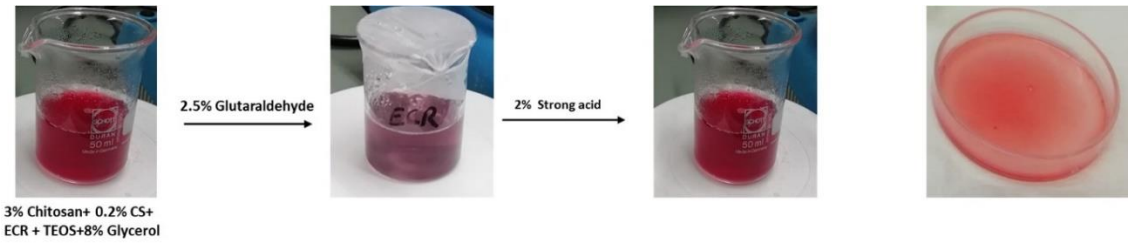

Fig.16 - ECR incorporated coloured membrane formed by regaining the lost colour of ECR by addition of a strong acid

The second method of incorporation of ECR after synthesis of membranes was found to be more successful. In this approach, the membranes prepared were immersed in 0.25mmol/L aqueous ECR solution for 24 hours prior to analysis. The transparent membranes became yellowish in colour due to the incorporation of ECR into the membrane, which in turn can produce violet colour when exposed to Al (III) ions as shown in Figure 17.

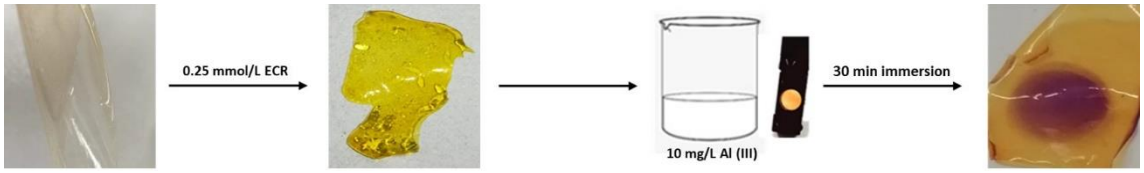

Fig.17 - Colour changes in the sensor membrane on incorporation of ECR (yellow) followed by immersion in Al (III) (violet) by using specially designed cuvette to hold the membrane

For the real time application of the developed membrane incorporated with ECR as an optical sensor for the detection of Al (III), it was necessary to optimize the immersion time in the aluminium cation containing solution, prior to optical analysis. In order to verify the optimal contact time of each membrane with the solution containing Al (III) ions, all the four types of membranes prepared were subjected to kinetics study separately, by immersion in 10 mg/L Al (III) in buffer solution of pH 5 and analysed using UV-Vis spectroscopy at regular time intervals. The spectra obtained for different types of membranes are presented in Figure 18.

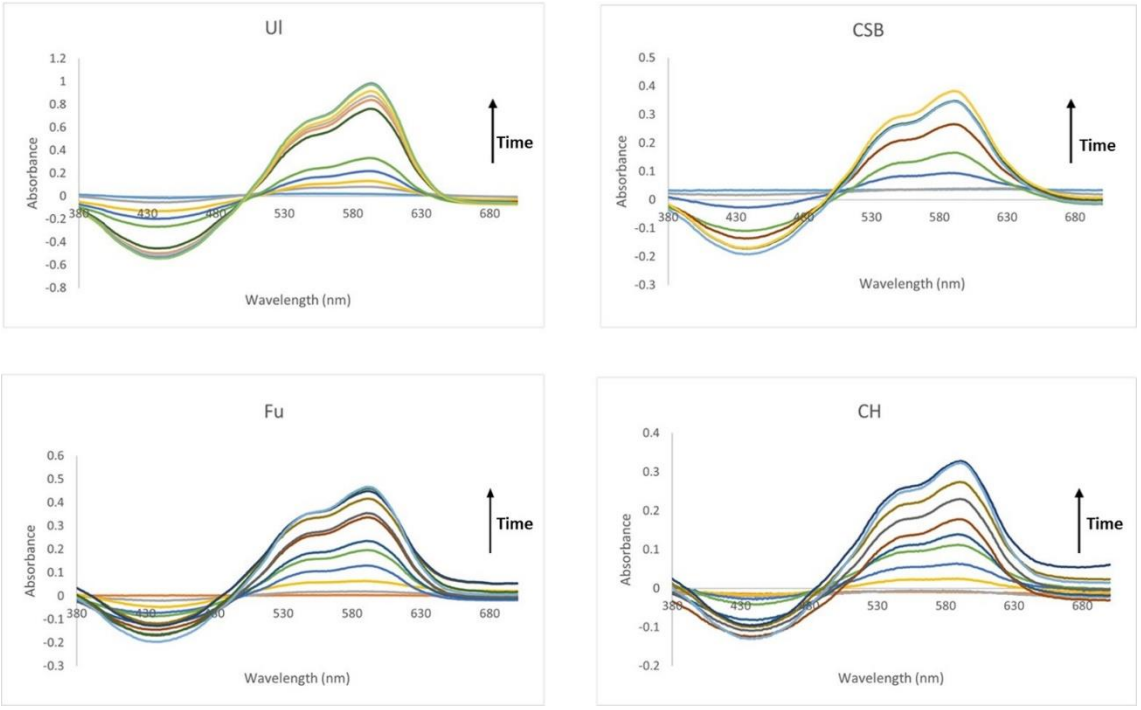

Fig.18 - Absorbance spectra of different membranes for kinetic studies

From the plot given in Figure 19, it can be inferred that the increase in the immersion time allows a greater number of aluminium ions to bind to ECR forming Al (III)-ECR complex. However, it is important to choose an optimal time of immersion which can give good optical signals for sensor applications. Despite not all signals showed to be stabilizing after 32 min, this time was set as compromise between sensitivity and analysis time, but it had to be tightly controlled. Hence, the time of immersion for this study was chosen to be 32 minutes.

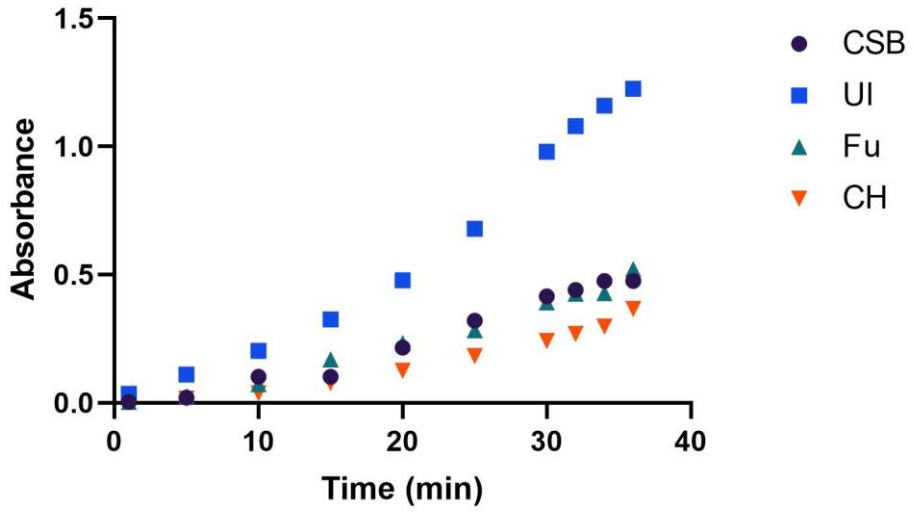

Fig.19 - Variation of the absorbance as a function of time in different types of membranes

This graph also reveals the superior performance of ulvan based membranes by giving clearly high absorbance when compared to other membranes (> two-fold at 32 min). Based on this result, the performance of different membranes as sensors for detection of Al (III) can be ranked in the order Ul>>CSB>Fu>CH. This trend was much as expected. From the information provided by the supplier, the extraction process of Ul required several steps of purification for the removal of aluminium from its naturally available form. This shows that Ulvans, by nature have great affinity towards aluminium. Also, CSB and Fu are expected to have better binding affinity to aluminium due to the presence of carboxylate and sulfonate groups present unlike CH.

4.3. Performance evaluation of the developed sensor membranes

The performance of the sensor membranes was evaluated using the spectral data obtained. For this, the ECR immobilised membrane was analysed in UV-Vis spectroscopy at a regular time interval of 32 minutes after immersion in 0.002 mol/L acetate buffer solution (pH 5), containing varying concentrations of Al (III) ions in the range of 1 to 20 mg/L. Figure 20 shows the absorption spectra of different types of sensor membranes, which are recorded at 380-700 nm range of wavelengths.

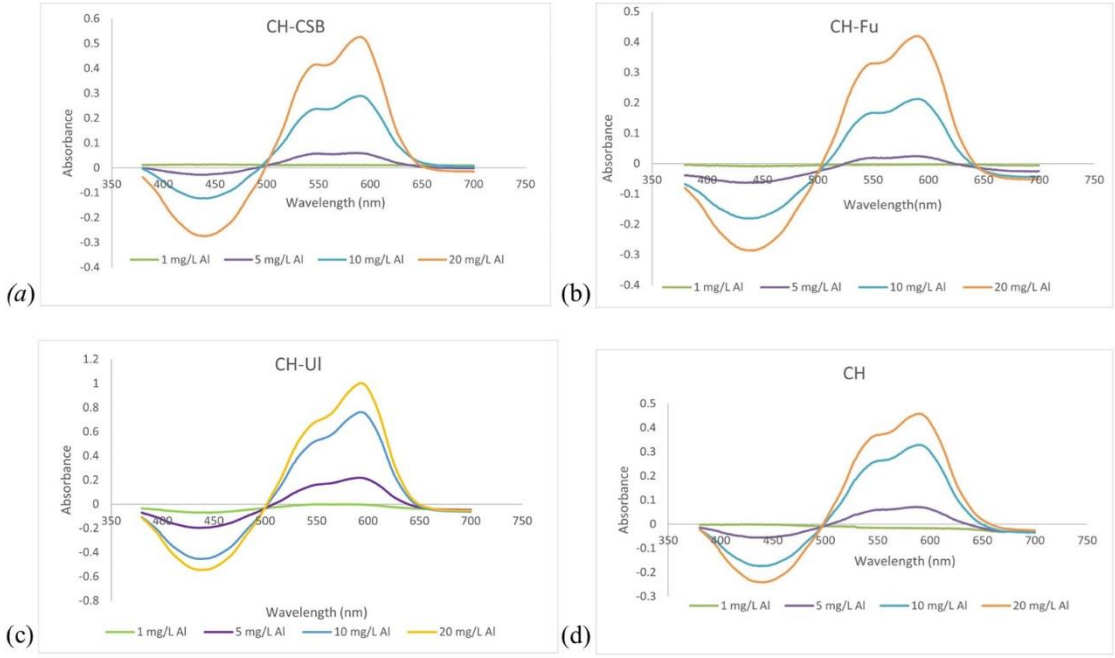

Fig.20 - Absorption spectra of the four types of sensor membranes for different concentrations of Al (III) at pH 5 (a) CH-CSB (b) CH-Fu (c) CH-UI (d) CH

The ECR immobilised membranes in the absence of Al (III) have a characteristic peak at around 450 nm. Upon complexation on exposure to Al (III) ions, the membrane changes its colour from yellow to violet resulting in the peak shift to higher wavelengths. In all the above cases shown in Figure 20, there are two absorption maxima at around 543 nm and 590 nm. But since the sensitivity at 590 nm is higher, this wavelength was

selected for measuring the response of the sensor towards Al (III). Similarly, a corresponding decrease in the absorption maxima of ECR at 450 nm can also be observed proportional to ECR-Al (III) complex formation represented at 590 nm.

4.4. Study of the effect of surfactants on the optical absorption behaviour of the sensor membranes

ECR is a good spectrophotometric reagent for the detection of Al (III) ions [4]. However, the spectrophotometric methods for the determination of aluminium based on binary complexes with triphenylmethane reagents like Eriochrome Cyanine R exhibit moderate sensitivity. The introduction of a third component [a long chain quaternary base (cationic surfactant)] to the binary system, leads to the formation of a ternary complex with advantageous properties. Such ternary systems are expected to be more sensitive than the spectrophotometric methods based on binary systems for the detection of metal ions [44]. Also, the expected red shift in the peak wavelength can give beneficial effects in terms of interferences. Hence, the effects of incorporation of cationic surfactants like N,N-dodecyl trimethyl ammonium bromide (DTAB) and cetyltrimethylammonium bromide (CTAB) on the sensitivity of ECR-Al (III) complexation on the membrane in acetate buffer environment (pH 5) were investigated in this study.

The surfactants CTAB and DTAB were incorporated into the membrane during the synthesis, as explained in the procedure in two different ratios (1:1 and 1:2 ECR-surfactant) and analysed in UV-Vis spectroscopy after immersion in 20 mg/L Al (III) solution. Figure 21 and 22 show the effect of incorporation of surfactants during the synthesis of membranes.

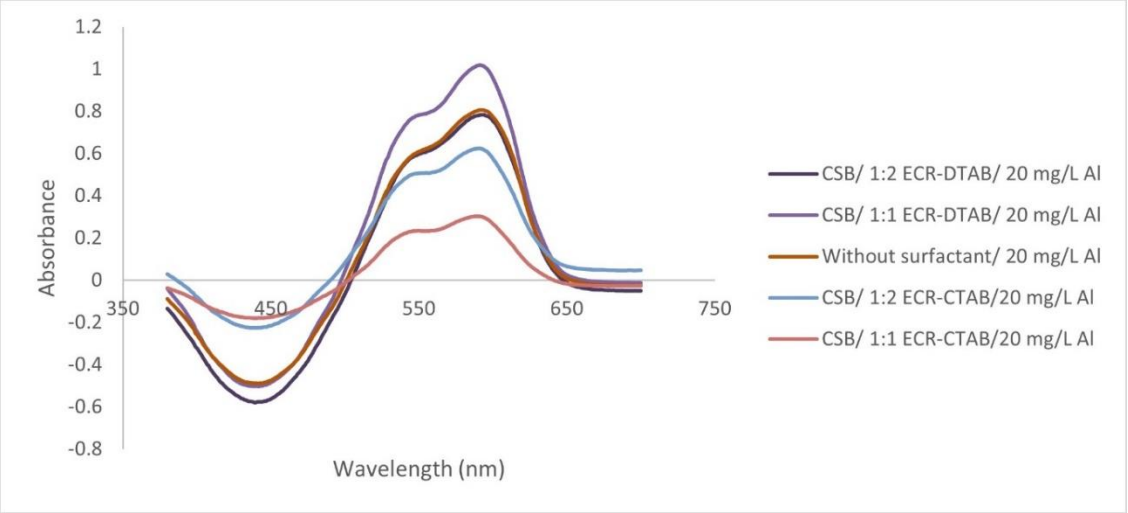

Fig.21 - Absorption spectra of CSB membrane incorporated with different surfactants (during the synthesis) upon immersion in 20 mg/L Al (III)

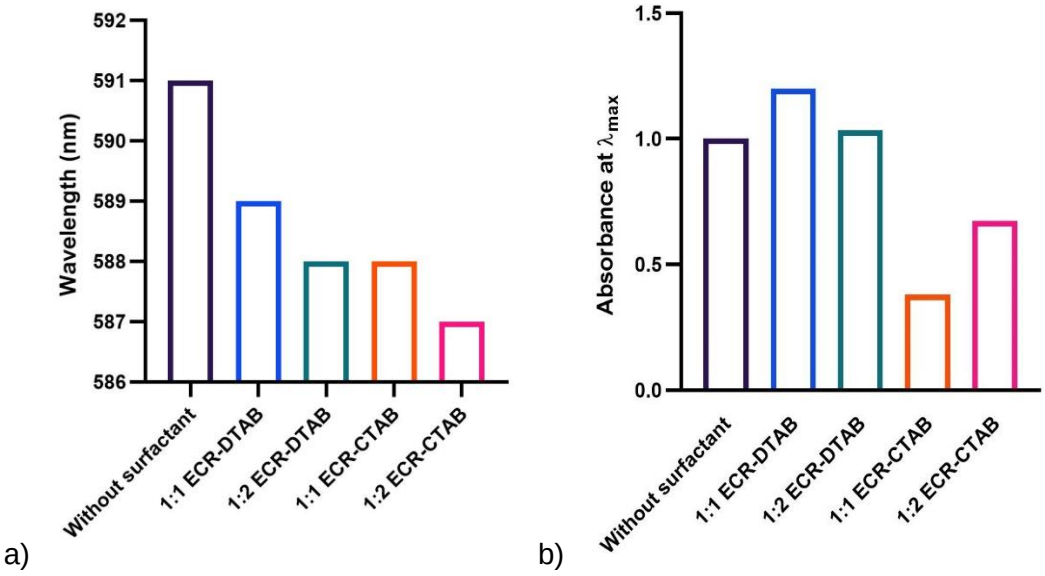

Fig.22 - Effect of incorporation of surfactants during the synthesis of membrane

As depicted in the graphs, no positive enhancement was observed in the performance of sensor membranes in comparison to the results obtained without the use of surfactant. In terms of wavelength, a blue shift was observed upon the addition of DTAB and CTAB. However, an increase in sensitivity was observed on addition of DTAB.

The second approach was the addition of surfactant after the synthesis of membrane. This was done by adding appropriate concentration of the surfactant to the sample solution to be analysed. The optimum concentration of the surfactants was chosen to be 1 mmol/L from the literature [45]. Initially, 0.5 mL of 1 mmol/L DTAB and CTAB were added separately to the samples containing varying concentrations of Al (III) ions in acetate buffer solution and the ECR incorporated membrane was immersed in it for a time period of 32 min. The membranes were then analysed using UV-Vis spectroscopy. The results of the peak positions obtained are shown in Figure 23.

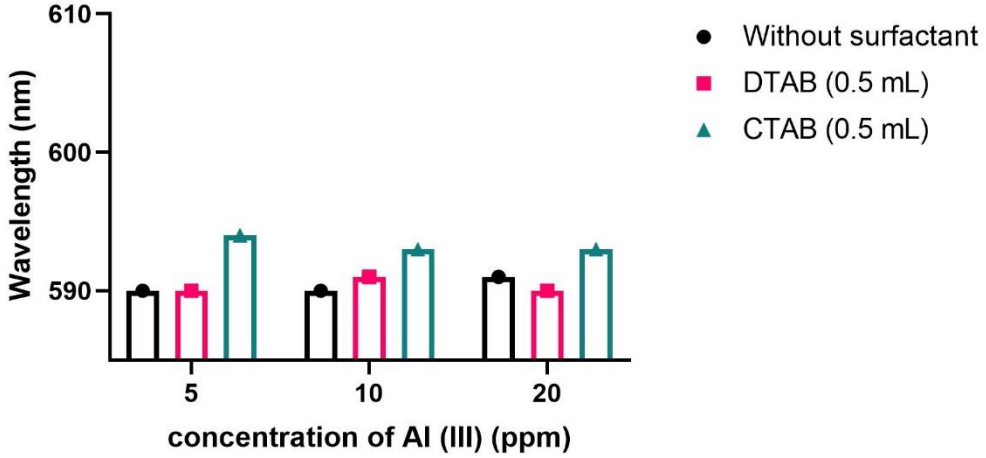

(a)

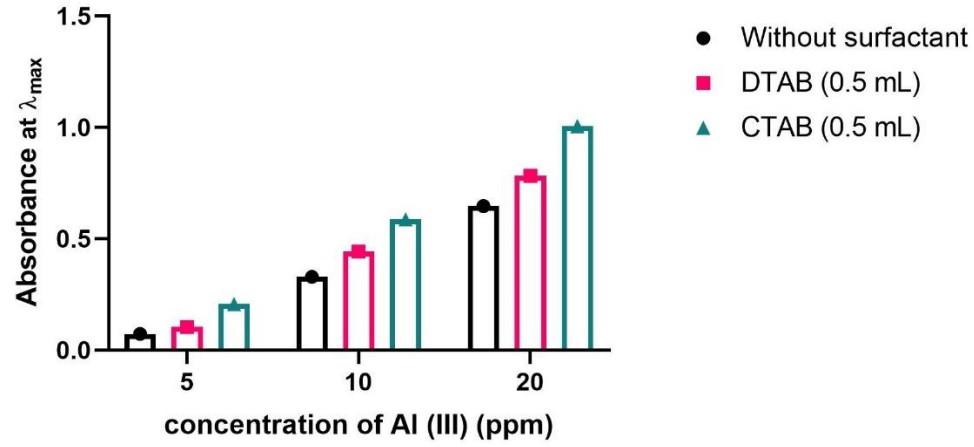

(b)

Fig.23 - Effect of incorporation of 0.5 mL surfactant 1 mmol/L (after the synthesis of membrane), demonstrated by the variation of (a) wavelength and (b) absorbance intensity as a function of concentration of Al (III) solution

This approach showed positive results as the membranes with surfactant, especially the one with CTAB, tends to show slight increase in the wavelength at all the three concentrations. An increase in the absorbance intensity upon addition of surfactant was also observed. However, the enhancement was not so pronounced in this case. Hence, a small modification was made in the above approach and analysed for the results. In this case, 2 mL of 1 mmol/L DTAB and CTAB were added. The results of the peak positions obtained are shown in the Figure 24.

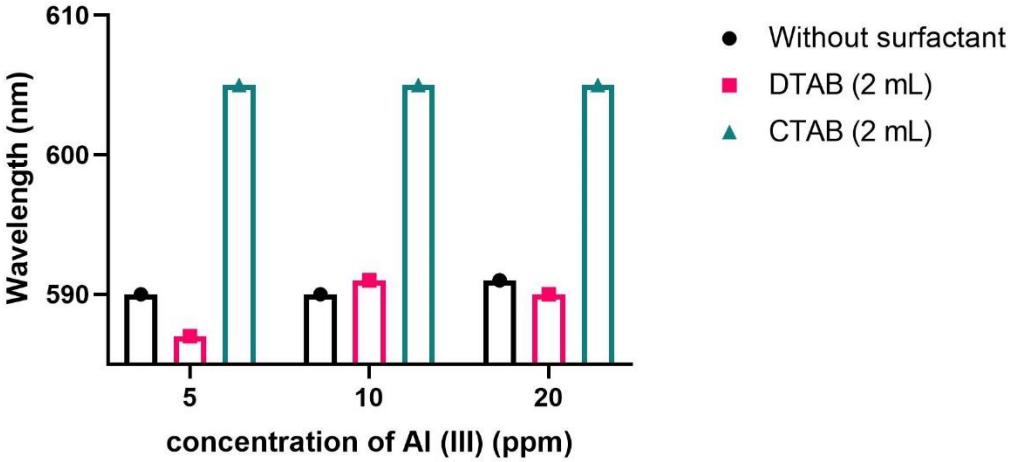

(a)

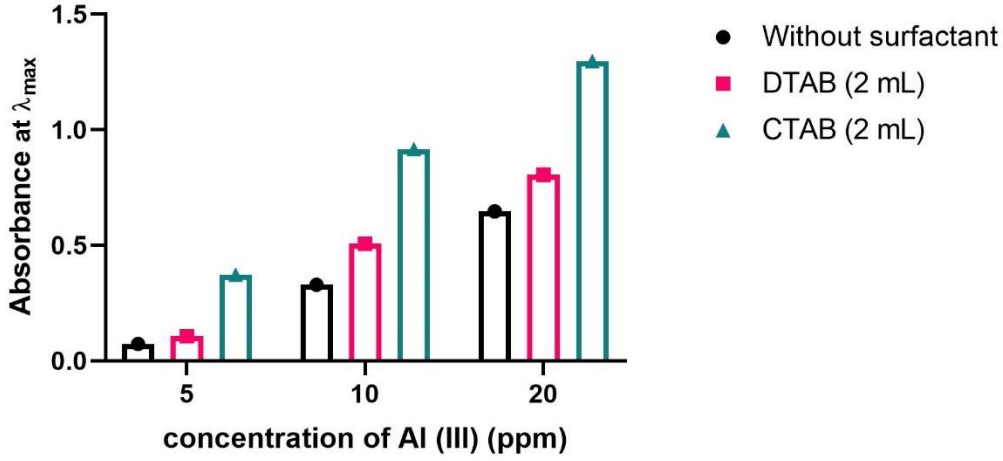

(b)

Fig.24 - Effect of incorporation of 2 mL surfactant 1 mmol/L (after the synthesis of membrane), demonstrated by the variation of (a) wavelength and (b) absorbance intensity as a function of concentration of Al (III) solution

It is evident from the graph that the incorporation of 2 mL of 1 mmol/L CTAB can significantly enhance the sensitivity of the sensor membrane. There is a clear red shift from around 590 nm to 605 nm. The absorption maxima at 590 nm corresponds to the binary ECR-Al (III) complex whereas the absorption maxima at 605 nm stands for the ternary ECR-Al (III)-CTAB complex formation. The colour change produced in this case was yellow to blue. The predicted increase in sensitivity can also be proved from the rise in absorbance intensity on addition of CTAB. Hence it is better to use 2 mL of 1 mmol/L CTAB instead of 0.5 mL of 1 mmol/L CTAB.

Since the incorporation of CTAB was found to be advantageous, the effect of CTAB on the optical absorption behaviour of all the four membranes were studied in the range of 1 to 20 mg/L with the addition of 2 mL of 1 mmol/L CTAB. Figure 25 shows the difference in spectra of CH-CSB membrane with and without the use of CTAB.

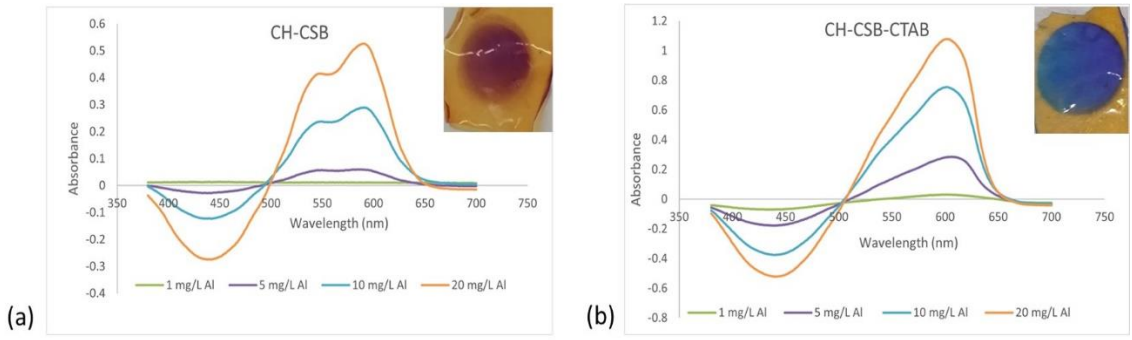

Fig.25 - Absorption spectra of CH-CSB membrane a) without CTAB b) with CTAB

The other types of membranes like Fu, Ul and CH based membranes were also analysed simultaneously with and without CTAB and the corresponding absorption spectra are given in Figure 26. A red shift in peak wavelength along with increase in absorbance intensity were observed in each case. It can also be noticed that Ul based membrane did not show superior performance in terms of sensitivity compared to other types of membranes, as expected. The reason for this is supposed to be related to the shell life of the membrane. The Ul membrane was analysed for the effect of CTAB, almost one month after its synthesis and the properties of the membrane might be affected with time. However, more studies are required to verify this assumption.

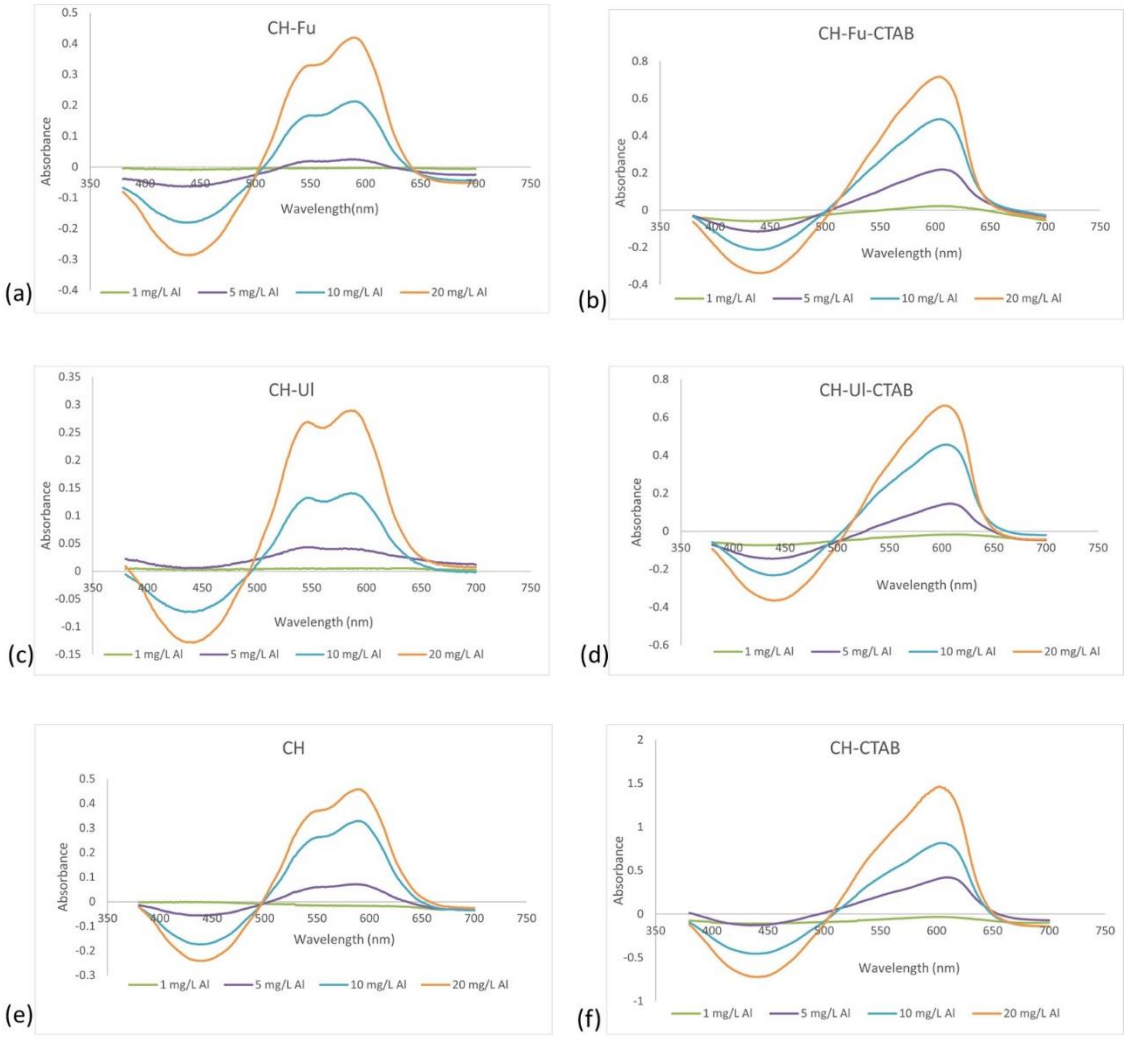

Fig.26 - Absorbance spectra of other membranes with and without CTAB (a) CH-Fu (b) CH-Fu-CTAB (c) CH-Ul (d) CH-Ul-CTAB (e) CH (f) CH-CTAB

Figure 27 shows that a clear red shift in peak wavelength occurs on addition of CTAB for every membrane at all concentrations analysed in the range of 1 to 20 mg/L. This property can be utilised to minimise the effect of interference caused by other species. Although further studies are required to verify this assumption. Similarly, CTAB addition has contributed to improvement of sensitivity of the membranes almost twice when compared to those without CTAB. This enhancement in sensitivity for different membranes analysed in the concentration range of 1 to 20 mg/L Al (III) can be seen in Figure 28. The overall results obtained confirm the positive impact of incorporation of CTAB on the sensor responses of all the membranes.

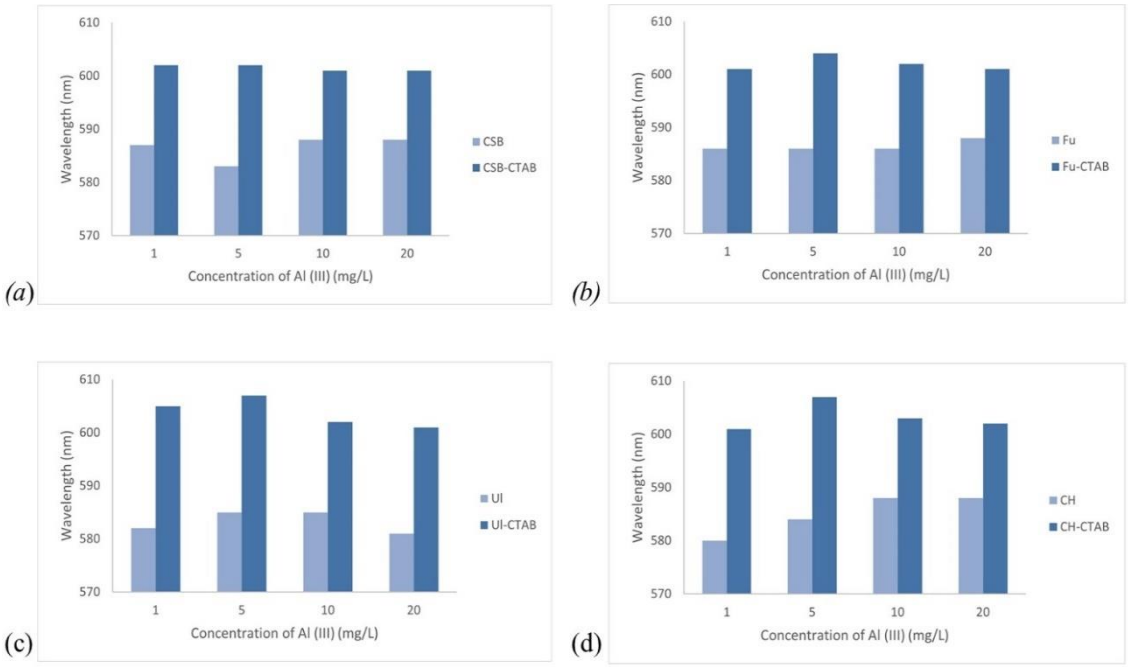

Fig.27 - Effect of CTAB on the peak wavelength shift for different sensor membranes (a) CH-CSB (b) CH-Fu (c) CH-UI (d) CH

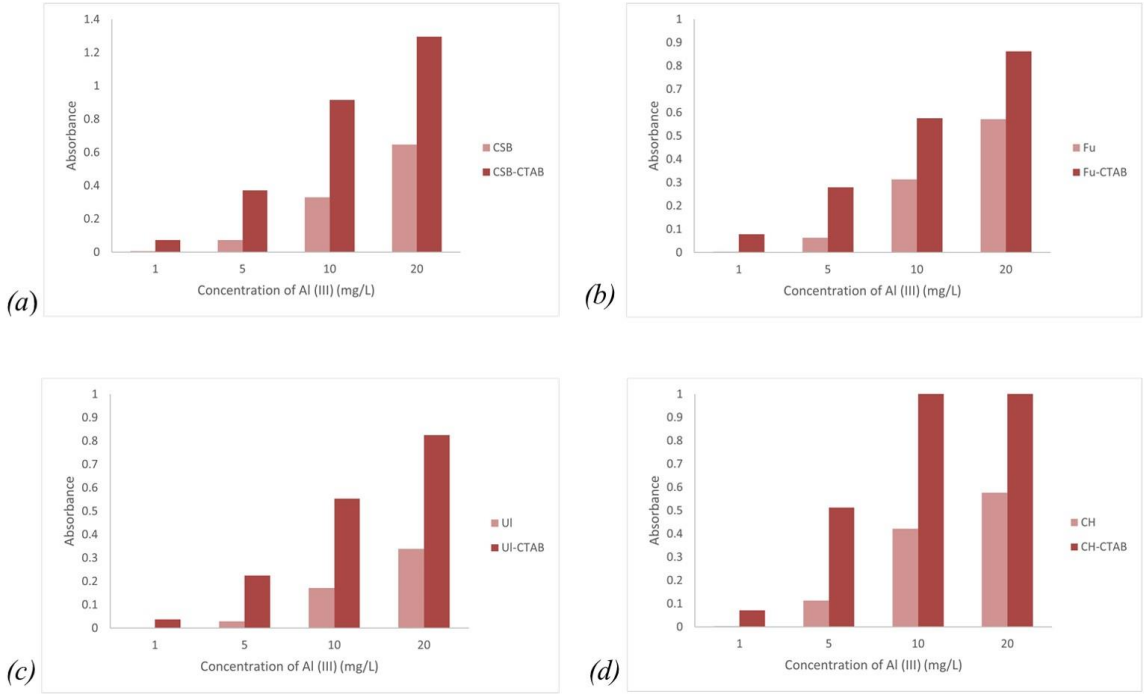

Fig.28 - Effect of CTAB on the sensitivity of different membranes (a) CH-CSB (b) CH-Fu (c) CH-UI (d) CH

4.5. Study of the effect of interfering species on the selectivity of sensor membranes

In practice, no sensor membranes have 100% selectivity to a particular metal ion**.** The sensor performance is likely to get affected by interfering species. In this case, Al (III) being the primary species of interest, the effect of possible interfering ions was studied in similar ways using UV-Vis analysis. Based on the literature [46], various interesting cationic and anionic species probable to interfere with aluminium like Cu (II), Fe (II), Fe(III), Cd (II), Pb (II), Cr (VI) and F^- were selected, as they were known to show interference with Al (III) in aqueous solutions. However, it might have a different behaviour when tested for membranes and hence it was important to analyse the effect of these interfering species in the sensor membranes prepared.

The study was carried out in CSB membranes, both in the presence and absence of CTAB. Initially the effect of these potential interfering species was individually examined. The spectra obtained when different interfering ions were individually analysed on the CSB membranes without the incorporation of CTAB are shown in Figure 29. This helps for easy visual identification of the potential interfering species. Al (III) shows a peak at 590 nm in CSB membranes in the absence of CTAB. Cu (II) was found to show high interference with Al (III) ions, showing a well-defined absorption peak at 574 nm, even at lower concentrations. Fe (II) can give interference with Al (III) from 20 mg/L and above. Cr (VI) tends to show a peak at 370 nm but does not interfere with Al (III) peak at 590 nm. However, Fe (III), Cd (II), Pd (II) and F^- have no significant interference with Al (III) at least in the concentration range 1 to 20 mg/L, as they do not have any peaks around 590 nm to interfere with Al (III).

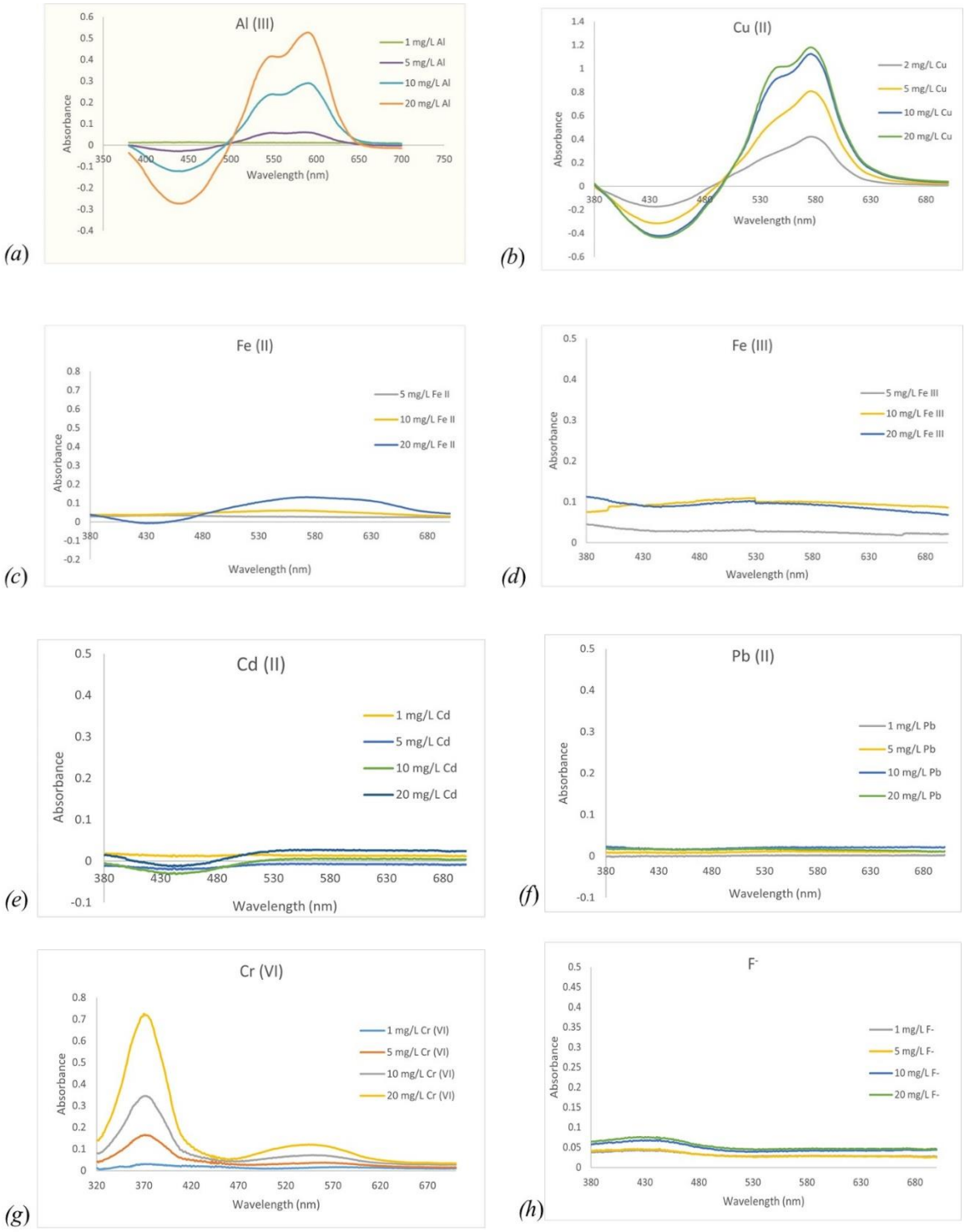

Fig.29 - Absorption spectra of CSB membranes on immersion in various interfering species, without CTAB (a) Al (III) (b) Cu (II), (c) Fe (II), (d) Fe (III), (e) Cd (II), (f) Pb (II), (g) Cr (VI) and (h) F^-

From the spectral data obtained, it is possible to determine the selectivity coefficient (K) for each interfering ion. From the single analyte measurements, admitting an independent behaviour for Al (III) and interferent, selectivity coefficient can be estimated using Equation 8.

$K_{Al,Int} = (A_{Int}/C_{int})/(A_{Al}/C_{Al})$ ……...Eq.8

where A_{Int} and A_{Al} stand for absorbance of interferent and aluminium at corresponding concentrations C_{Int} and C_{Al}.

For the analysis of CSB membranes without CTAB, all the absorbance values were measured at the peak wavelength 590 nm. The K values obtained for CSB membranes in the absence of CTAB are given in Table 1. The lower the K value, the lesser is the interference and more selective is the membrane towards Al (III).

Interfering Species	***Selectivity ($K_{Al,Int}$)***
Cu (II)	1.414
Fe (II)	0.085
Fe (III)	0.079
Cd (II)	0.007
Pb (II)	0.032
Cr (VI)	0.081
F^-	0.064

Table 1 - Selectivity coefficient values of different interfering species

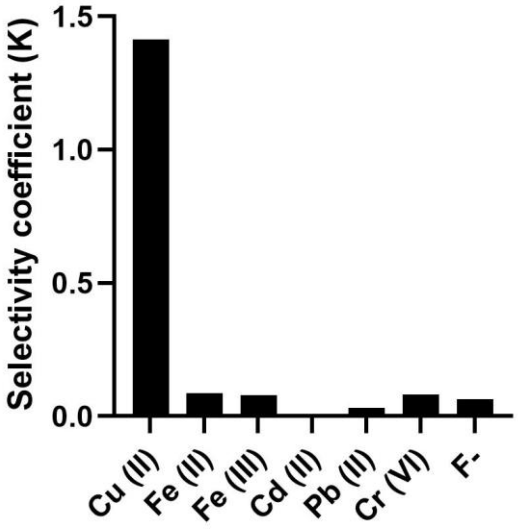

Fig.30 - Selectivity plot

From Table 1 and Figure 30, Cu (II) can, as expected, be identified as a severe interference to Al (III) using the membrane under study with almost 1.5 times higher selectivity than Al (III). Cu (II) being an intermediate ligand, has good affinity with ECR and known to form $Cu(ECR)_2$ complexes [47]. However, other factors like permeability, ionic radius etc might also be contributing factors to the high interference of copper in this proposed Al (III) sensor membrane. It should also be noted that the K values of other non-interfering species might be an overestimated value due to the errors in baseline corrections.

However, the use of CTAB is expected to contribute to minimise the effect of interfering species. Hence the membranes incorporated with CTAB were analysed to study the effect on interference. The spectra obtained when Al (III) and Cu (II) were individually analysed on the CSB membranes incorporated with CTAB are shown in Figure 31.

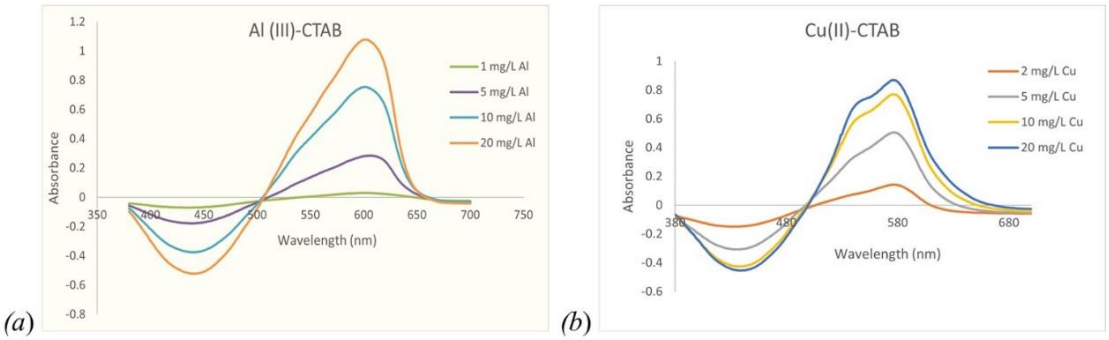

Fig.31 - Absorption spectra of CSB membranes incorporated with CTAB on immersion in (a) Al (III) (b) Cu (II)

It was found that no change in peak wavelength, 575 nm in the case of Cu (II) with CTAB whereas Al (III) peak wavelength changes from 590 nm to 604 nm in the presence of CTAB. From the spectral data obtained for CSB membranes with and without CTAB, the sensitivity response of the sensor membranes on exposure to Al (III) and Cu (II) can be shown in a plot of variation of absorbance intensity as a function of concentration of metal ions given in Figure 32. It was observed that the sensitivity of Cu (II) decreases while that of Al (III) increases upon addition of CTAB. The combined effect of this change in sensitivity along with the red shift for Al (III) upon CTAB addition is expected to minimise the effect of interference from Cu (II) to the proposed Al (III) sensor membrane. Both these effects are illustrated in the absorption spectra given in Figure 33.

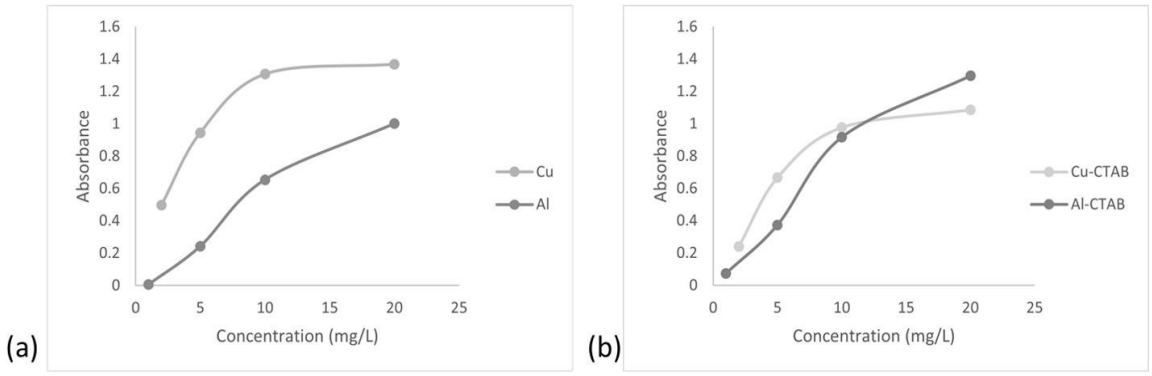

Fig.32 - Sensitivity of sensor membrane towards Al (III) and Cu (II) (a) without CTAB (b) with CTAB

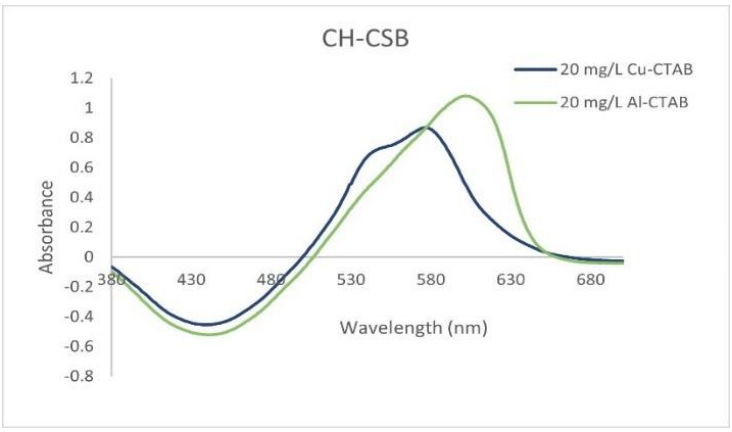

Fig.33 - Absorption spectra of CSB membranes incorporated with CTAB on immersion in Al (III) and Cu (II) individually at 20 mg/L concentration

The selectivity coefficient K for Cu (II) in CSB membranes incorporated with CTAB was estimated to be 0.40, where all absorbance values were measured at Al peak value 604 nm. The new K value for Cu (II) is much lower than the K value obtained for CSB membranes without CTAB, suggesting lesser interference of Cu (II) in the Al (III) sensor membrane. It is also notable that the K value for Cu (II) can be even smaller as 0.24 at wavelength 624 nm, though at the expense of sensitivity of the sensor.

Cd (II) and Pd (II) gave no peaks in the presence of CTAB as in the absence of CTAB as given in Figure 34. It would have been interesting to know the effect of CTAB in the detection of Fe (II), Fe (III) and Cr (VI). Unfortunately, they have not yet been analysed due to time constraints.

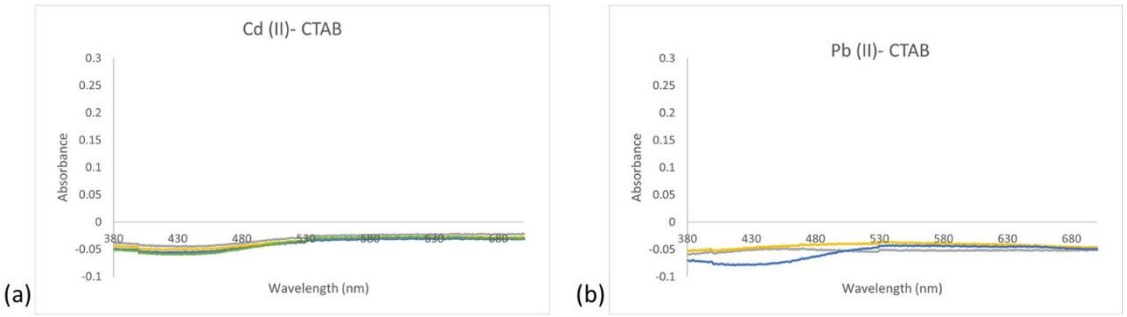

Fig.34 - Absorption spectra of CSB membranes incorporated with CTAB on immersion in (a) Cd (II) (b) Pb (II)

However, the real effect of interfering species on the selectivity of the sensor membrane can be analysed only by immersing the membrane in a solution containing a mix of Al (III) ions and the interfering species, both in the presence and absence of CTAB. This is due to the reason that, both species when introduced together in a solution, compete to form complex with ECR in the membrane, and hence we can study the actual effect of interfering species on the Al (III) sensor membrane. This study will be continued though, unfortunately could not be included in this dissertation.

Conclusion

This thesis presented mainly four types of Al (III) sensor membranes made from marine based biopolymers namely chitosan, chondroitin sulfate, fucoidan and ulvans, for the detection of aluminium cation by complexation with the chromophore, eriochrome cyanine R (ECR). Membranes with sulfated biopolymers showed better performance than the membrane with only chitosan, possibly due to the sulfate and the carboxylate groups present. The effect of incorporation of surfactants like CTAB and DTAB in the sensor performance was studied using UV-Vis spectroscopy. It was found that the use of 2 mL of 1 mmol/L CTAB can significantly enhance the sensitivity of the sensor membranes. They could also give a red shift in the peak wavelength.

The selectivity of the proposed Al (III) membranes was also evaluated by testing for interference from other metal ions. Cu (II) was found to cause severe interference with Al (III) cation. Since CTAB was found to have more specific effect on ECR-Al (III) complexation compared that of Cu (II), the use of CTAB is expected to be beneficial to minimise the copper interference. However, the real outcome can be confirmed only after further analysis of the sensor membranes in a sample containing multiple interfering ions in addition to Al (III).

It was also observed that the membrane properties start to deteriorate after a few weeks and some membranes analysed without considering this aspect, was found to show low sensitivity than expected. Hence it is necessary to monitor the stability and lifetime of different types of membranes under study. We plan to continue the studies on these important aspects. The future scope of study also includes molecular imprinting.

References

[1] G. L. Turdean, 'Design and Development of Biosensors for the Detection of Heavy Metal Toxicity', *Int. J. Electrochem.*, vol. 2011, pp. 1–15, 2011.

[2] N. K. Srivastava and C. B. Majumder, 'Novel biofiltration methods for the treatment of heavy metals from industrial wastewater', *J. Hazard. Mater.*, vol. 151, pp. 1–8, 2008.

[3] R. B. Thompson, B. P. Maliwal, V. L. Feliccia, C. A. Fierke, and K. McCall, 'Determination of Picomolar Concentrations of Metal Ions Using Fluorescence Anisotropy: Biosensing with a "Reagentless" Enzyme Transducer', Analytical Chemistry, vol. 70, p. 7, 1998.

[4] H. Khajehsharifi, A. Solhjoo, and M. M. Bordbar, 'Design of an Optical Sensor for Aluminium(III) Determination Based on Immobilization of Eriochrome Cyanine R on a Triacetylcellulose', Iranian Journal of Analytical Chemistry, vol. 3, pp.145-152, 2016.

[5] A. Hulanicki', S. Geab, and F. Ingman, 'Chemical Sensors - Definitions and Classifications', Pure & Appl. Chem, vol. 63, pp. 1247-1250, 1991.

[6] M. Bosch, A. Sánchez, F. Rojas, and C. Ojeda, 'Recent Development in Optical Fiber Biosensors', *Sensors*, vol. 7, pp. 797–859, 2007.

[7] I. Oehme and O. S. Wolfbeis, 'Optical sensors for determination of heavy metal ions', *Mikrochimica Acta*, vol. 126, pp. 177–192, 1997.

[8] H. Liu *et al.*, 'Application of Biodegradable and Biocompatible Nanocomposites in Electronics: Current Status and Future Directions', vol. 9, pp. 950, 2019.

[9] V. K. Thakur and S. I. Voicu, 'Recent advances in cellulose and chitosan based membranes for water purification: A concise review', *Carbohydrate Polymers*, vol. 146, pp. 148–165, 2016.

[10] D. Teng, ‘From chitin to chitosan’, *Chitosan Based Hydrogels Functions and Applications*, pp. 2–33, 2011.

[11] T. J. Brown and M. B. Emelko, ‘Chitosan and metal salt coagulant impacts on Cryptosporidium and microsphere removal by filtration’, *Water Research*, vol. 43, pp. 331–338, 2009.

[12] M. N. R. Kumar, ‘A review of chitin and chitosan applications’, *React. Functional Polymers*, vol. 46, pp. 1–27, 2000.

[13] S. Y. Park, K. S. Marsh, and J. W. Rhim, ‘Characteristics of different molecular weight chitosan films affected by the type of organic solvents’, *J. Food Science*, vol. 67, pp. 194–197, 2002.

[14] R. Clark and B. Averbach, ‘The Mechanical Properties of Chitosan Membranes’, in *OCEANS’78*, pp. 82–86, 1978.

[15] A. Anitha *et al.*, ‘Chitin and chitosan in selected biomedical applications’, *Prog. Polymer Science*, vol. 39, pp. 1644–1667, 2014.

[16] V. R. A. Ferreira *et al.*, ‘Metal cation sorption ability of immobilized and reticulated chondroitin sulfate or fucoidan through a sol-gel crosslinking scheme’, *Mater. Today Commun.*, vol. 8, pp. 172–182, 2016.

[17] C. Malavaki, S. Mizumoto, N. Karamanos, and K. Sugahara, ‘Recent Advances in the Structural Study of Functional Chondroitin Sulfate and Dermatan Sulfate in Health and Disease’, *Connect. Tissue Res.*, vol. 49, pp. 133–139, 2008.

[18] J. Vázquez, I. Rodríguez-Amado, M. Montemayor, J. Fraguas, M. González, and M. Murado, ‘Chondroitin Sulfate, Hyaluronic Acid and Chitin/Chitosan Production Using Marine Waste Sources: Characteristics, Applications and Eco-Friendly Processes: A Review’, *Mar. Drugs*, vol. 11, pp. 747–774, 2013.

[19] V. R. A. Ferreira *et al.*, 'Cationic imprinting of Pb(II) within composite networks based on bovine or fish chondroitin sulfate', *J. Mol. Recognit.*, vol. 31, pp. e2614, 2018.

[20] M. N. Rodrigues, M. B. Oliveira, R. R. Costa, and J. F. Mano, 'Chitosan/Chondroitin Sulfate Membranes Produced by Polyelectrolyte Complexation for Cartilage Engineering', *Biomacromolecules*, vol. 17, pp. 2178–2188, 2016.

[21] B. Li, F. Lu, X. Wei, and R. Zhao, 'Fucoidan: Structure and Bioactivity', Molecules, vol. 13, pp. 1671-1695, 2008.

[22] I. P. S. Fernando, 'Advances in functionalizing fucoidans and alginates (bio)polymers by structural modifications_ A review', *Chem. Eng. J.*, vol.35, pp. 33-38, 2019.

[23] T. Hahn, S. Lang, R. Ulber, and K. Muffler, 'Novel procedures for the extraction of fucoidan from brown algae', *Process Biochem.*, vol. 47, pp. 1691-1698, 2012.

[24] K.-Y. Lu, 'Development of a new type of multifunctional fucoidan-based nanoparticles for anticancer drug delivery', *Carbohydr. Polym.*, vol. 165, pp. 410-420, 2017.

[25] G. Toskas *et al.*, 'Ulvan and ulvan/chitosan polyelectrolyte nanofibrous membranes as a potential substrate material for the cultivation of osteoblasts', *Carbohydr. Polym.*, vol. 89, pp. 997–1002, 2012.

[26] M. Dash *et al.*, 'Biofunctionalization of ulvan scaffolds for bone tissue engineering', *ACS Appl. Mater. Interfaces*, vol. 6, pp. 3211–3218, 2014.

[27] M. Lahaye and A. Robic, 'Structure and functional properties of ulvan, a polysaccharide from green seaweeds', *Biomacromolecules*, vol. 8, pp. 1765–1774, 2007.

[28] L.-A. Tziveleka, E. Ioannou, and V. Roussis, ‘Ulvan, a bioactive marine sulphated polysaccharide as a key constituent of hybrid biomaterials: A review’, *Carbohydr. Polym.*, vol. 218, pp. 355–370, 2019.

[29] A. R. Ganesan, M. Shanmugam, and R. Bhat, ‘Producing novel edible films from semi refined carrageenan (SRC) and ulvan polysaccharides for potential food applications’, *Int. J. Biol. Macromol.*, vol. 112, pp. 1164–1170, 2018.

[30] V. Hlavacek and J. A. Puszynski, ‘Chemical Engineering Aspects of Advanced Ceramic Materials’, *Ind. Eng. Chem. Res.*, vol. 35, pp. 349–377, 1996.

[31] B. Kaur, N. Kaur, and S. Kumar, ‘Colorimetric metal ion sensors – A comprehensive review of the years’, *Coord. Chem. Rev.*, vol. 358, pp. 13-69, 2018.

[32] M. Jaishankar, T. Tseten, N. Anbalagan, B. B. Mathew, and K. N. Beeregowda, ‘Toxicity, mechanism and health effects of some heavy metals’, *Interdiscip. Toxicol.*, vol. 7, pp. 60–72, 2014.

[33] D. J. Hawke, H. K. J. Powell, and S. L. Simpson, ‘Equilibrium modelling of interferences in the visible spectrophotometric determination of aluminium (III): comparison of the chromophores chrome azurol S, eriochrome cyanine R and pyrocatechol violet, and stability constants for eriochrome cyanine R-aluminium complexes’, *Anal. Chim. Acta*, vol. 319, pp. 305–314, 1996.

[34] S. Bahrani, M. Ghaedi, M. J. K. Mansoorkhani, A. Asfaram, A. A. Bazrafshan, and M. K. Purkait, ‘Ultrasonic assisted dispersive solid-phase microextraction of Eriochrome Cyanine R from water sample on ultrasonically synthesized lead (II) dioxide nanoparticles loaded on activated carbon: Experimental design methodology’, *Ultrason. Sonochem.*, vol. 34, pp. 317–324, 2017.

[35] S. G. Kazarian and K. L. A. Chan, 'Applications of ATR-FTIR spectroscopic imaging to biomedical samples', *Biochim. Biophys. Acta BBA - Biomembr.*, vol. 1758, pp. 858–867, 2006.

[36] J. Greener, B. Abbasi, and E. Kumacheva, 'Attenuated total reflection Fourier transform infrared spectroscopy for on-chip monitoring of solute concentrations', *Lab. Chip*, vol. 10, pp. 1561, 2010.

[37] W. Mäntele and E. Deniz, 'UV–VIS absorption spectroscopy: Lambert-Beer reloaded', *Spectrochim. Acta. A. Mol. Biomol. Spectrosc.*, vol. 173, pp. 965–968, 2017.

[38] Y. Nur, E. Rohaeti, and L. K. Darusman, 'Optical Sensor for the Determination of Lead (II) Based on Immobilization of Dithizone onto Chitosan-Silica Membrane', *Indones. J. Chem.*, vol. 17, pp. 7, 2017.

[39] K. M. Abdel-Gawad, A. F. Hifney, M. A. Fawzy, and M. Gomaa, 'Technology optimization of chitosan production from Aspergillus niger biomass and its functional activities', *Food Hydrocoll.*, vol. 63, pp. 593–601, 2017.

[40] S. Shankar and J.-W. Rhim, 'Preparation of sulfur nanoparticle-incorporated antimicrobial chitosan films', *Food Hydrocoll.*, vol. 82, pp. 116–123, 2018.

[41] T. Crouzier and C. Picart, 'Ion Pairing and Hydration in Polyelectrolyte Multilayer Films Containing Polysaccharides', *Biomacromolecules*, vol. 10, pp. 433–442, 2009.

[42] S. J. Lim, W. M. Wan Aida, M. Y. Maskat, S. Mamot, J. Ropien, and D. Mazita Mohd, 'Isolation and antioxidant capacity of fucoidan from selected Malaysian seaweeds', *Food Hydrocoll.*, vol. 42, pp. 280–288, 2014.

[43] N. A. Azmi, S. H. Ahmad, and S. C. Low, 'Detection of mercury ions in water using a membrane-based colorimetric sensor', *RSC Adv.*, vol. 8, pp. 251–261, 2018.

[44] Z. Marczenko and M. Jarosz, ‘Formation of ternary complexes of aluminium with some triphenylmethane reagents and cationic surfactants’, *The Analyst*, vol. 107, p. 1431, 1982.

[45] W. Siriangkhawut, S. Tontrong, and P. Chantiratiku, ‘Quantitation of Aluminum Content in Waters and Soft Drinks by Spectrophotometry Using Eriochrome Cyanine R’Research’, *J. Pharm. Biol. Chem. Sci.*, vol. 4, pp. 1156–1161, 2013.

[46] 'Description of test kit for Eriochrome Cyanine R method 8326 for Aluminium', Hach Company, 2018.

[47] N. A. J. M. Sommerdijk, A. Poppe, C. A. Gibson, and J. D. Wright, ‘Unexpected complexation behaviour of a sol–gel immobilised dye: the development of an optical copper(II) sensor’, *J. Mater. Chem.*, vol. 8, pp. 565–567, 1998.